Revisiting the Chemistry and Photophysics of 3-(N -Methylpyridinium-4-yl)Coumarins for Designing "Covalent-Assembly" and "Molecular Disassembly" Fluorescent Probes

Vincent Gaumerd, Kévin Renault, Pierre-yves Renard, Anthony Romieu

ChemPhotoChem

Research Article
doi.org/10.1002/cptc.202300324

Chemistry Europe
European Chemical Societies Publishing

www.chemphotochem.org

Revisiting the Chemistry and Photophysics of 3-(*N*-Methylpyridinium-4-yl)Coumarins for Designing "Covalent-Assembly" and "Molecular Disassembly" Fluorescent Probes

Vincent Gaumerd[+],[a] Kévin Renault[+],*[a, b] Pierre-Yves Renard,[c] and Anthony Romieu*[a]

The constant need for high-performance aniline- or phenol-based fluorophores suitable for the construction of activity-based fluorescent probes, led us to study both synthesis and photophysics of C3-*N*-methylpyridinium-4-yl substituted 7-(dialkylamino)/7-hydroxycoumarins. Indeed, in the field of photoactive organic molecules, the positively charged *N*-alkylpyridinium-4-yl groups are often used as acceptor units to dramatically impact spectral features through promoting intramolecular charge transfer (ICT) processes. They are also known as effective water-solubilizing and mitochondria targeting moieties. The poor fluorescence efficiency of cationic 7-hydroxycoumarin derivatives in aqueous physiological conditions was highlighted and rationalized by the predominance of a neutral quinonoid form in such buffer medium. The ability of the excited singlet state (S_1) of this neutral species to undergo intersystem crossing (ISC) to triplet state (T_1) was partly supported by phosphorescence measurements of singlet oxygen. We also took advantage of green-emissive properties of 7-(diethylamino)-3-(*N*-methylpyridinium-4-yl)coumarin to successfully design and validate a novel small-molecule fluorescent probe for the detection of alkaline phosphatase (ALP), based on the "covalent-assembly" principle. A practical use of *ortho*-formylated 7-hydroxy-3-(*N*-methylpyridinium-4-yl)coumarin was next considered with the synthesis of a Fe(III)-salen complex whose the potential as a "molecular disassembly" probe for fluorogenic sensing of pyrophosphate (PPi) anion was assessed.

Introduction

In the burgeoning field of activity-based fluorescence sensing,[1] coumarin dyes, mainly those bearing an electron-donating group (EDG) at the C7 position (*i.e.*, (dialkyl)amino or hydroxyl group), play a central role as an effective signaling unit to construct quality analyte-responsive probes.[2] Even if their valuable spectral features (broad Stokes' shift and good-to-high fluorescence quantum yields under physiological conditions) are often solely obtained within the short wavelength region of the visible spectrum (*i.e.*, blue-cyan or green spectral range), a myriad of practical (bio)analytical applications using coumarin derivatives as fluorescent reporters have been reported.[3] More recently, the pronounced need for longer wavelength fluorophores facilitating detection in complex matrices or biological media, has promoted the emergence of coumarin-based near-infrared probes.[4] In this context, various molecular design strategies have been implemented to readily achieve marked red-shift of absorption/emission wavelengths of coumarin scaffold. The preferred one is based on the simultaneous introduction of an EDG at the C7 site and an electron-withdrawing group (EWG) at the C3 position. This strengthens the "push-pull" effect and intramolecular charge transfer (ICT) characteristic, thus decreasing HOMO-LUMO energy gap.[4a] The most popular electron acceptors suitable for this purpose are benzopyrylium, indolenium, and multiple-cyano (hetero)cyclic moieties including dicyanoisophorone, dicyanomethylene-4*H*-pyran, and tricyanofuran scaffolds, often introduced at the C3 site through a dimethine bridge. Surprisingly, less attention has been paid to electron-withdrawing quaternarized aromatic *N*-heterocyclic substituents (*e.g.*, *N*-alkylpyridinium or quinolinium moiety) directly attached to the coumarin core. This is confirmed by the few number of publications dealing with the synthesis, photophysics and/or sensing applications of pyridinium-decorated 7-(dialkylamino)/7-hydroxycoumarins.[5] The pioneering work of the Wolfbeis group deserves to be pointed

[a] *V. Gaumerd,[+] Dr. K. Renault,[+] Prof. A. Romieu*
Institut de Chimie Moléculaire de l'Université de Bourgogne, UMR 6302, CNRS
Université de Bourgogne
9, Avenue Alain Savary
21000 Dijon (France)
E-mail: kevin.renault@curie.fr
anthony.romieu@u-bourgogne.fr

[b] *Dr. K. Renault[+]*
CNRS UMR9187, Inserm U1196, Chemistry and Modeling for the Biology of Cancer Institut Curie, Université PSL, 91400 Orsay (France)

[c] *Prof. Dr. P.-Y. Renard*
Univ Rouen Normandie, INSA Rouen Normandie, CNRS, Normandie Univ, COBRA UMR 6014, INC3M FR 3038, 76000 Rouen (France)
1, Rue Tesnière
76821 Mont-Saint-Aignan Cedex (France)

[+] *These authors contributed equally to this work.*

[**] *A previous version of this manuscript has been deposited on a preprint server (DOI: 10.26434/chemrxiv-2023-n9vwf).*

Supporting information for this article is available on the WWW under https://doi.org/10.1002/cptc.202300324

out since it discloses the first synthesis and some spectral features (and their pH dependence) of 7-hydroxy-3-(*N*-methylpyridinium-x-yl)coumarins (x = 2, 3 or 4).[6] However, to the best of our knowledge, this study was not extended to the assessment of these phenols as fluorogenic reporters in the popular "OFF-ON" probe design strategy based on protection-deprotection of 7-OH group, especially for the detection of biorelevant analytes (*e.g.*, enzymes). Interestingly, but outside the context of fluorophores, the chemistry of 7-(dialkylamino)-3-(*N*-methylpyridinium-x-yl)coumarins (x = 2 or 4) was intensively studied by the Henkel company in order to identify cationic dyes suitable for dyeing keratinic fibers and thus usable in preparations for temporary coloring the hair.[7] Lastly, more recently, the ability of 7-(diethylamino)-3-(*N*-methylpyridinium-x-yl)coumarins (x = 2, 3 or 4) to act as AND logic gate fluorescent probes responsive to both pH and polarity changes typical of mitochondria in cancer cells, was assessed but no conclusive results were obtained.[8] Within this context, we wished to revisit the chemistry of 7-(diethylamino)- and 7-hydroxy-3-(*N*-methylpyridinium-4-yl)coumarins **1** and **2** in order both to deepen the understanding of their peculiar spectral properties and to evaluate their potential in fluorogenic biosensing of reactive analytes (Figure 1, top). In addition to its electron-withdrawing character, the *N*-methylpyridinium-4-yl group also acts as an effective water-solubilizing moiety without compromising cell permeability.[9] Its mitochondria targeting ability[10] and high binding affinity to macrocyclic hosts such as curcubit[n]urils (CB[n]) have also facilitated the development of "smart" fluorescent probes with better performances for practical sensing/imaging applications.[11] Herein, we report a novel synthetic route towards the two cationic fluorophores **1** and **2** and *ortho*-formyl derivative **3**. A comprehensive photophysical study notably involving the determination of their fluorescence properties in various aq. media, ground-state pKa determination (for phenol derivatives) and phosphorescence measurement of singlet oxygen ($^1O_2$) production was carried out to delineate their performances as light-emitting reporters and/or type II photosensitizers (PSs). The practical utility of these coumarin derivatives was also explored through the design of two distinct fluorescent probes/chemodosimeters responsive to either alkaline phosphatase (ALP), an important diagnostic enzyme, or biologically relevant pyrophosphate (PPi) anion respectively. Two remerging reaction-based strategies recently highlighted for their positive attributes to achieve higher detection performances in terms of limit of detection (LOD) and analyte selectivity, have been used. For ALP sensing,

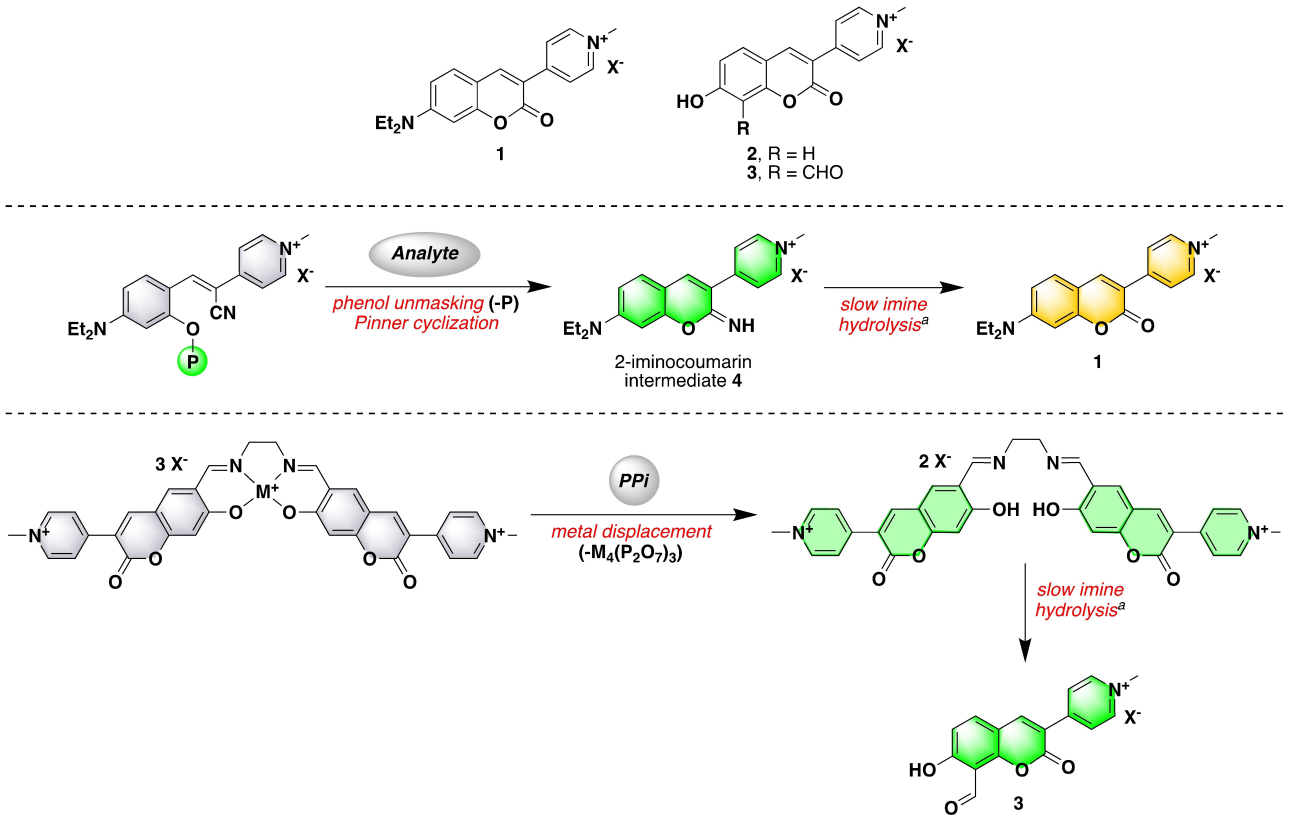

Figure 1. Structures of 3-(*N*-methylpyridinium-4-yl)coumarins studied in this work (top). Potential practical activity-based sensing applications explored in this work: (middle) "covalent-assembly" fluorescent probes for the detection of enzymes through *in situ* sequential formation of (2-imino)coumarins **4** then **1**; (bottom) "molecular disassembly" fluorescent probes for the detection of PPi anion through the hypothetical release of coumarin **3**. [M = Fe(III) cation but Al(III) cation can be also used for producing a fluorescence ratiometric output, P = recognition moiety for the targeted enzyme, PPi = pyrophosphate anion, X^- = iodide or trifluoroacetate anion]. [a] Please note: For clarity, water molecules involved in such reactions and released ammonia and 1,2-ethylenediamine molecules are omitted. Please note: the color of the structure indicates approximately the spectral range of its emission: grey = non-fluorescent, green = emission of (2-imino)coumarins **3** and **4**, faded green = emission of salen ligand assumed to be less fluorescent than **3**, orange = emission of coumarin **1**.

"covalent-assembly" probe design principle (rationalized by Anslyn and Yang)[12] was preferred in order to study the ability of this enzyme to trigger *in situ* synthesis of 7-(diethylamino)-3-(*N*-methylpyridinium-4-yl)coumarin **1** under aqueous conditions, and through a domino process involving Pinner cyclization followed by spontaneous imine hydrolysis of intermediate **4** (Figure 1, middle). The selective detection of PPi anion was based on the disassembly of a Fe(III)-salen complex (*i.e.*, metal displacement followed by hydrolysis of the bis-Schiff base bridging ligand to release a fluorescent salicylaldehyde derivative, Figure 1, bottom). Our working assumption is inspired by the recent contribution of the Zelder group.[13] As the intent is to evaluate the versatility of this approach, particularly its possible extension to phenol-based fluorophores whose *ortho*-formylation leads to enhancement of their fluorescence brightness.

Results and Discussion

Synthesis of cationic coumarins using latent C-nucleophile 2-(N-methylpyridinium-4-yl)acetonitrile

On the basis of works mainly focused on the preparation of various 3-heteroaryl-7-hydroxycoumarin dyes, reported by the Wolfbeis group,[6] we designed a simple and convenient synthetic route towards cationic coumarins **1** and **2**, through a domino Knoevenagel condensation/Pinner cyclization strategy, ended by acidic hydrolysis of 2-iminocoumarin intermediates (Scheme 1). The successful implementation of this reaction sequence is facilitated by the commercial availability of 2-(pyridin-4-yl)acetonitrile (hydrochloride salt form) whereas the major challenge may be related to the purification of the positively-charged hydrophilic compounds. First, 2-(pyridin-4-yl)acetonitrile was quaternized with methyl iodide (7 equiv.), in the presence of TEA (1.2 equiv.) in dry MeCN at 50 °C. In order to avoid a tedious and time-consuming purification by reversed-phase flash-chromatography followed by freeze-drying, 2-(*N*-methylpyridinium-4-yl)acetonitrile **5** was readily isolated by Et_2O precipitation, as a mixture with TEA hydrochloride salt (in a 1:1 proportion as determined by ^{1}H-NMR). Since this latter ammonium salt is assumed to not negatively interfere during the domino process, the precipitated latent *C*-nucleophile was directly reacted with commercial 4-(diethylamino)salicylaldehyde or 2,4-dihydroxybenzaldehyde, in the presence of piperidine (catalytic amount), in EtOH at room temperature, to give the corresponding *N*-methylpyridinium-decorated 7-(diethylamino)/7-hydroxy-2-iminocoumarins **6** and **7**. Final aqueous acid hydrolysis of their imine moiety (by adding aq. aq. HCl, and heating under reflux for 1–2 h) resulted in the desired 3-(*N*-methylpyridinium-4-yl)coumarins. We managed to isolate **1** (iodide salt) in a pure form, by Et_2O precipitation, washings and free-drying (isolated yield: 33 %). Yet, such purification protocol failed to allow isolation of the phenolic coumarin **2** in a pure form. As an alternative, after work-up (neutralization) of the acidic reaction mixture, the crude product was subjected to semi-preparative RP-HPLC purification (using aq. 0.1 % TFA and MeCN as eluents) and pure **2** was recovered as TFA salt (isolated yield: 65 %, based on TFA mass = 39.5 % (1.45 molecules)). In order to consider the synthesis of PPi-responsive Fe(III)-salen complexes derived from 7-hydroxycoumarin derivative **2** (Figure 1, bottom), *ortho*-formylation of this latter compound is required. Indeed, the availability of a salicylaldehyde moiety enables to achieve Schiff

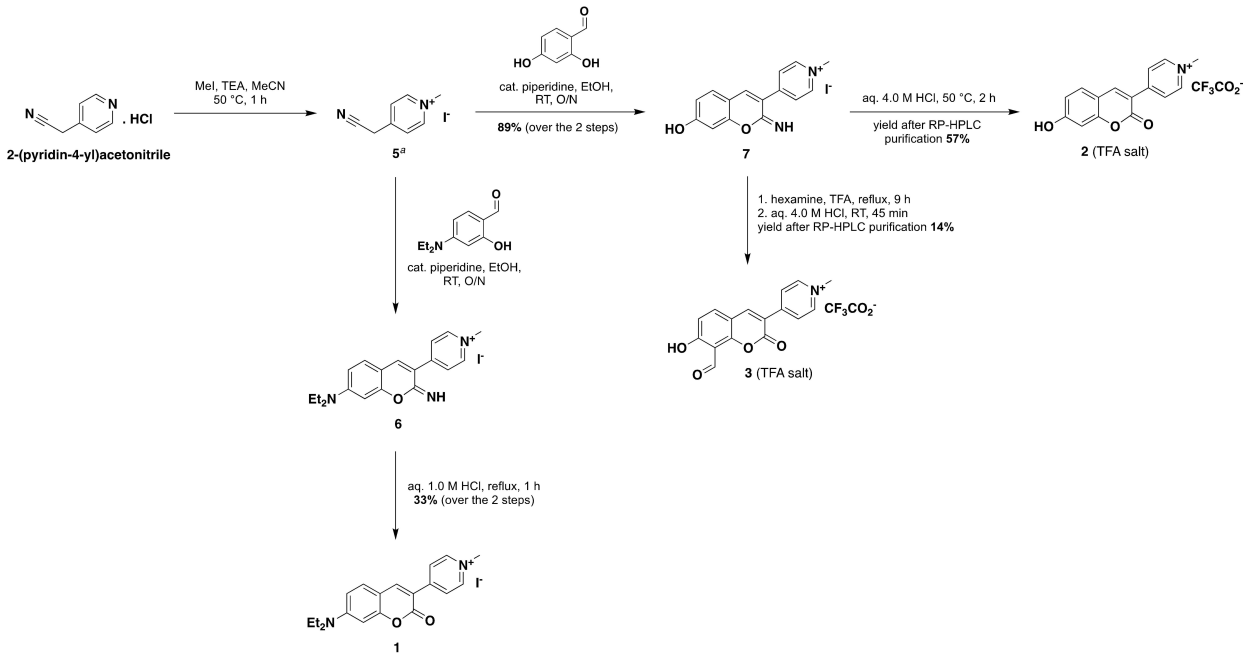

Scheme 1. Synthesis of 3-(*N*-methylpyridinium-4-yl)coumarins **1**–**3**. [a] Please note: this compound was isolated as a 1:1 mixture with TEA.HCl salt. [O/N = overnight, RT = room temperature, TEA = triethylamine, TFA = trifluoroacetic acid].

base condensations with the corresponding 1,2-diamine. Due to the lack of solubility of this cationic coumarin in common organic solvents (*e.g.*, DCM, THF, …), the choice of experimental conditions for its formylation is somewhat limited. For instance, the practical implementation of the Casnati-Skattebøl (*i.e.*, paraformaldehyde, $MgCl_2$, TEA, in dry THF)[14] and Rieche (*i.e.*, dichloromethyl methyl ether, $TiCl_4$, in dry DCM)[15] reactions is not possible. Guided by our previous work on *ortho*-formylation of sulfonated 7-hydroxycoumarins,[16] the Duff reaction occurring in a polar protic medium (*i.e.*, TFA as solvent which was found to be effective to dissolve pyridinium-containing coumarins), was chosen. Furthermore, due to strong acidic conditions employed for this formylation reaction, this was simpler and more straightforward to use 7-hydroxy-2-iminocoumarin intermediate **7** as starting phenolic compound. Thus, treatment of **7** with hexamine (2.3 equiv.) in refluxing TFA for 9 h, followed by a brief hydrolysis under acidic conditions (aq. 4.0 M HCl, 45 min at room temperature) provided the targeted salicylaldehyde-containing fluorophore **3**. Its isolation in a pure form (and as TFA salt) was achieved by semi-preparative RP-HPLC (isolated yield: 14%, based on TFA mass = 48.0% (2.3 molecules)). The structures of 3-(*N*-methylpyridinium-4-yl)coumarins **1**–**3** were confirmed by detailed measurements, including ESI-MS and NMR spectroscopic analysis (see the Supporting Information). The purity of these cationic coumarin samples was confirmed by RP-HPLC analyses with UV-vis detection at different wavelengths, and found to be suitable for an accurate and reliable determination of their photophysical properties.

Photophysical properties of 3-(N-methylpyridinium-4-yl)coumarins

The primary goal of this comprehensive photophysical study is to have a clear idea of the brightness of both 3-(*N*-methylpyridinium-4-yl)coumarins **1** and **2** under buffered neutral conditions, in order to confirm their potential use as reporters in biosensing applications. That's why we initially conducted spectral measurements in phosphate buffer (PB, 100 mM, pH 7.4). Next, further characterizations were also achieved in polar and non-polar organic solvents namely EtOH and $CHCl_3$. All spectroscopic data are gathered in Table 1, and the corresponding electronic absorption, excitation, and emission spectra are available in Figure 2 or in the Supporting Information. As expected, whatever the solvent used, the UV-vis absorption spectrum of 7-(diethylamino)-3-(*N*-methylpyridinium-4-yl)coumarin **1** displays a broad (full-width half maximum ($\Delta\lambda_{1/2max}$) within the range 53–67 nm) and intense band centered within the range 475–500 nm range as a well-known feature of push-pull molecules that exhibit a strong ICT

Table 1. Photophysical properties of 3-(*N*-methylpyridinium-4-yl)coumarins at 25 °C.

Cmpd[a]	Solvent	Abs max[b] [nm]	Em max [nm]	Stokes shift [cm^{-1}]	ε [$M^{-1}cm^{-1}$]	Φ_F[c] [%]
1	PB (pH 7.4)	475	558	3 131	48 500	2%
	Tris.HCl buffer (pH 8.0)	475	558	3 131	48 900	1.5%
	EtOH	482	561	2 921	49 300	27%
	$CHCl_3$	500	547	1 718	58 000	25%
2	PB (pH 7.4)	447	_[d]	_[d]	39 900	-[d]
	Acetate buffer (pH 4.3)	379	467	4 972	31 400	1%
	EtOH	398, 490	476, 535[e]	4 117 1 716	_[f]	_[f]
	$CHCl_3$	405, 545[g]	477 _[g]	3 727 _[g]	_[f]	_[f]
3	PB (pH 7.4)	440	520	3 496	57 800	1%
	EtOH	380, 475	535[h]	7 624 2 361	_[f]	_[f]
	$CHCl_3$	386, 534	_[i]	_[i]	39 950 _[f]	_[f]

[a] Stock solutions (1.0 mg/mL) of fluorophores/probes prepared in DMSO. [b] Only 0–0 band of the S_0-S_1 transition of coumarin unit is reported. [c] Determined using coumarin 153 (C153, $\Phi_F = 38\%$ in EtOH as a standard) except for **2** in acetate buffer (7-hydroxycoumarin, $\Phi_F = 76\%$ in PB, pH 7.4)[17]. [d] No significant fluorescence emission except for high concentrated solutions (> 5.0 μM, Ex/Em maxima = 373/480 nm) not suitable for determination of relative quantum yield. [e] Very weak emission only observed upon Ex at 490 nm. [f] Non-linear relationships that prevent determination of molar extinction coefficients and relative fluorescence quantum yields. [g] No emission upon Ex at 550 nm. [h] A shoulder is observed at 470 nm. [i] Red-edge phenomenon, explained by the synergistic effect of ESIPT and ICT, leads to a complex emission profile (*e.g.*, two emission maxima at 458 nm and 525 nm and a shoulder at ca. 565 nm upon Ex within the range 360–420 nm, and red-shift Em spanning the range 536–554 nm upon Ex within the range 460–520 nm. See Supporting Information for the corresponding fluorescence emission spectra.

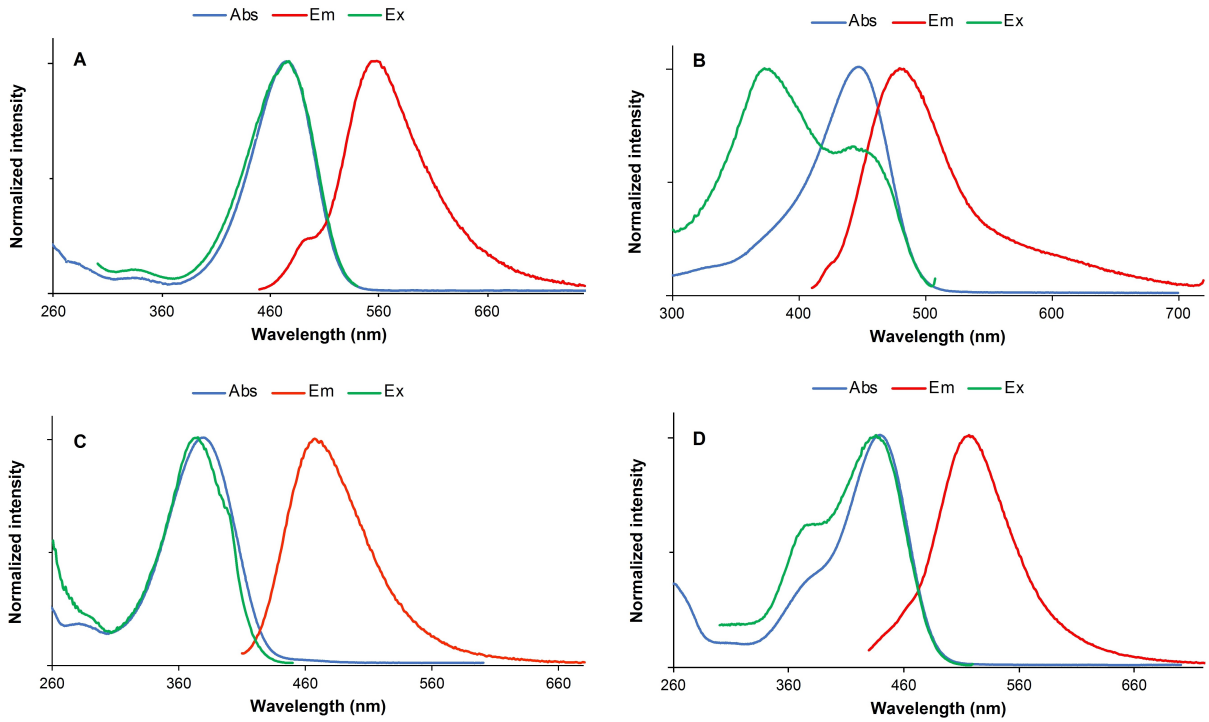

Figure 2. Normalized UV-visible absorption, fluorescence emission and excitation spectra of 3-(*N*-methylpyridinium-4-yl)coumarins in aqueous buffers at 25 °C: (A) coumarin **1** in PB (100 mM, pH 7.4), (B) phenolic coumarin **2** in PB, (C) phenolic coumarin **2** in acetate buffer (100 mM, pH 4.3), (D) phenolic coumarin **3** in PB. See Supporting Information for parameters used to record spectra. Please note: phenolic coumarin **2** was assumed to be non-fluorescent but we recorded its excitation/emission spectra using a highly-concentrated solution (> 5.0 μM), out of the range typically used for determination of relative fluorescence quantum yields (0.1–0.5 μM).

character. Upon excitation, **1** exhibits a yellow-orange fluorescence emission centered at 558 nm in PB (Figure 2A), 561 nm in EtOH and 547 nm in $CHCl_3$ respectively. A low fluorescence quantum yield of 2% was determined in PB using coumarin 153 as reference ($\Phi_F = 38\%$ in EtOH),[17] in agreement with the occurrence of non-radiative twisted ICT (TICT) process known to readily dissipate the excited state energy. This behavior as well as the influence of solvent polarity were perfectly rationalized by Liang *et al.* through theoretical calculations.[8] Indeed, fluorescence quantum yields in organic solvents are expected to be higher because **1** has a lower charge separation and exhibits weaker interactions with solvent molecules in media less polar than water. In our case, fluorescence quantum yields were found to be close to 25% and no significant difference was noted between EtOH and less polar $CHCl_3$. This unexpected result may be explained by the use of a different excitation wavelength (420 nm and 450 nm respectively) to get full emission spectra suitable for an accurate determination of the area under the curves. However, fluorescence lifetime measurements through time correlated single photon counting (TCSPC) method have confirmed the hypothesis of a longer emissive excited state S_1 of **1** in $CHCl_3$ ($\tau = 1.9$ ns (55%) and 2.8 ns (20%) *vs.* 1.4 ns in EtOH and 1.5 ns in PB) For the phenolic counterpart **2**, the UV-vis curve is characterized by a very intense maximum absorption at 440 nm and a pronounced shoulder centered at 380 nm (Figure 2B). The longer wavelength band is interpreted as the spectral signature of the anionic form of 7-hydroxycoumarin **2** (*i.e.*, phenolate form **8**) and supported by the phenol ground-state pKa value of 6.7 determined by drawing pH-dependent absorption curves (see Supporting Information for raw and fitted curves). Conversely, the blue-shifted shoulder is assigned to the minor phenol form. Surprisingly and in contrast with the common spectral behavior of 7-hydroxycoumarin derivatives, no significant fluorescence emission was detected in PB at pH 7.5 except if measurements were achieved within a concentration range not relevant for the determination of a relative quantum yield (*i.e.*, > 5.0 μM, saturation of PMT detector of our spectrofluorimeter). This suggests that the phenolate form **8** is not an emissive species at physiological pH. The excitation spectrum also supports this hypothesis because the major emissive species is the phenol form whose excitation maximum is centered at 373 nm. In order to definitely confirm this, further spectral measurements were achieved in acetate buffer (100 mM, pH 4.3). Under these acidic aqueous conditions, a blue-green fluorescence unveiling was observed (emission centered at 467 nm) and a fluorescence quantum yield of 1% was determined using 7-hydroxycoumarin as reference ($\Phi_F = 76\%$ in PB, pH 7.4).[18] The perfect matching between excitation and absorption profiles confirms: (1) the protonated state of the emissive species (phenol form), and (2) the lack of non-emissive aggregates (*i.e.*, H-type homodimers) known to negatively impact brightness (Figure 2C), thus illustrating the positive effect of pyridinium moiety to impart to this fluorophore remarkable water solubility and resistance to self-aggregation. As initially proposed by Wolfbeis and Marhold[6] and confirmed

by the recent study of Hu *et al.* with *N*-methylquinolinium phenol vinyl conjugate **4NT**[19] (Figure 3, middle), the lack of fluorescence properties of the phenolate form of these push-pull structures bearing an *N*-alkylpyridinium or quinolinium moiety as EWG, is explained by the predominance in solution of the neutral quinonoid form (*i.e.*, merocyanine-type structure). The excited state S_1 of this latter one is prone to undergo ISC to populate low-lying triplet state T_1. In order to confirm this hypothesis, we assumed that part of such T_1 energy should be transferred to molecular oxygen (*i.e.*, triplet oxygen $^3O_2$) to produce detectable singlet oxygen ($^1O_2$). Using a single channel short-wave infrared (SWIR) detector (800-1550 nm) based on Indium-Gallium-Arsenic (InGaAs) semiconductor and cooled with liquid nitrogen, we managed to detect phosphorescence of $^1O_2$ centered around 1275 nm,[20] produced by merocyanine-type form **9** (Figure 3, top). The recording of exploitable phosphorescence spectra was only possible in deuterated chloroform ($CDCl_3$) that minimizes non-radiative deactivation of $^1O_2$ strongly favored by X–H oscillators (X = N, O),[21] and thus increases lifetime of this ROS (9.4 ms *vs.* 220 µs in $CHCl_3$) (Figure 4). However, we were aware that in this medium, the formation of neutral quinonoid form **9** would not be really favored and no quantitative measurement (*i.e.*, determination of singlet oxygen quantum yield using zinc(II) tetraphenylporphyrin (ZnTPP) as reference, $\Phi_\Delta = 72\%$ in $CHCl_3$)[22] was possible. Thus, we tried to perform such measurements in $CDCl_3$ containing 1% TEA. Under these non-aqueous basic conditions, quantitative conversion of **2** into its merocyanine-type form **9** was observed (pink color visible to the naked eye, absorption maximum around 550 nm) but no phosphorescence was detected because $^1O_2$ is readily quenched by this added tertiary amine.[23] As a final attempt, we used phosphate buffered saline (PBS, pH 7.4) prepared in heavy water (D_2O) as measuring medium but the $^1O_2$ lifetime remains to short (67 µs)[24] to properly visualize phosphorescence emission of this ROS. Furthermore, a comparison of the ability of 3-(*N*-methylpyridinium-4-yl)coumarins **1** and **2** to produce $^1O_2$, has clearly shown that both derivatives are able to partly transfer its T_1 excited energy to molecular oxygen. This is indirect evidence that ISC is operative in these push-pull molecules. In the case of **1**, the presence of iodide as the counter-ion of *N*-methylpyridinium-4-yl moiety may promote this photophysical process through external heavy atom effect.[25] Following the clever approach recently published by Hu *et al.* to disrupt such undesired spectral behavior at physiological pH,[19] we have considered the synthesis of *ortho*-formylated derivative **3** (*vide supra*) in order to determine its photophysical properties in PB. Contrary to its parent 7-hydroxycoumarin **2**, this phenol-based fluorophore was found to be fluorescent in this buffer with an emission maximum centered at 520 nm and a relative quantum yield of 1% ($\tau = 1.2$ ns). In this case, the excitation spectrum displays a major band centered at 436 nm perfectly superimposed with absorption curve (Figure 2D), thus suggesting the presence of an emissive species whose electronic structure is related to that of phenolate form **10**, not that of merocyanine-type form **11** (Figure 3, bottom). The low phenol ground-state pKa value found to be equal to 5.4 (see Supporting Information for raw and fitted curves) supports this assumption. We hypothesized that the formyl group adjacent to phenol/phenolate, compels an electronic movement limited to the salicylaldehyde moiety leading after proton abstraction from aqueous buffer to emissive electronic structure **12**. This latter

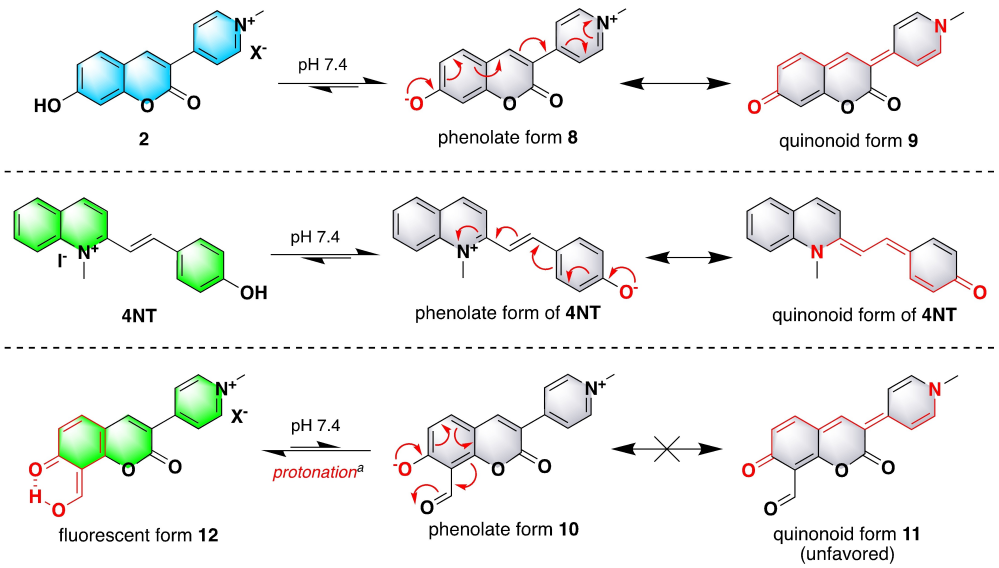

Figure 3. (Top) Proposed equilibrium to rationalize the lack of fluorescence of 7-hydroxycoumarin **2** in phosphate buffer (PB, 100 mM, pH 7.4); (middle) Similar equilibrium proposed by Hu *et al.* to rationalize the lack of fluorescence of *N*-methylquinolinium phenol vinyl conjugate **4NT** in cosolvent-buffer mixtures (PB, 20 mM, pH 7.4 with DMSO or MeCN in variable proportions);[19,57] (bottom) Proposed equilibrium to rationalize the emissive ability of 8-formyl-7-hydroxycoumarin **3** in phosphate buffer (PB, 100 mM, pH 7.4). [a] We assume that proton is abstracted from aqueous buffer. Indeed, due to the low ground state pKa value of phenol (5.4), it is quite unlikely that an intramolecular proton transfer directly occurs within the structure of 8-formyl-7-hydroxycoumarin **3** prior its deprotonation at pH 7.5 to give phenolate form **10**. Please note: the color of the structure indicates approximately the spectral range of its emission: grey = non-fluorescent, blue = emission of phenol form of **2** observed in acetate buffer (100 mM, pH 4.3), green = emission of 8-formyl-7-hydroxycoumarin **3** observed in PB (100 mM, pH 7.4).

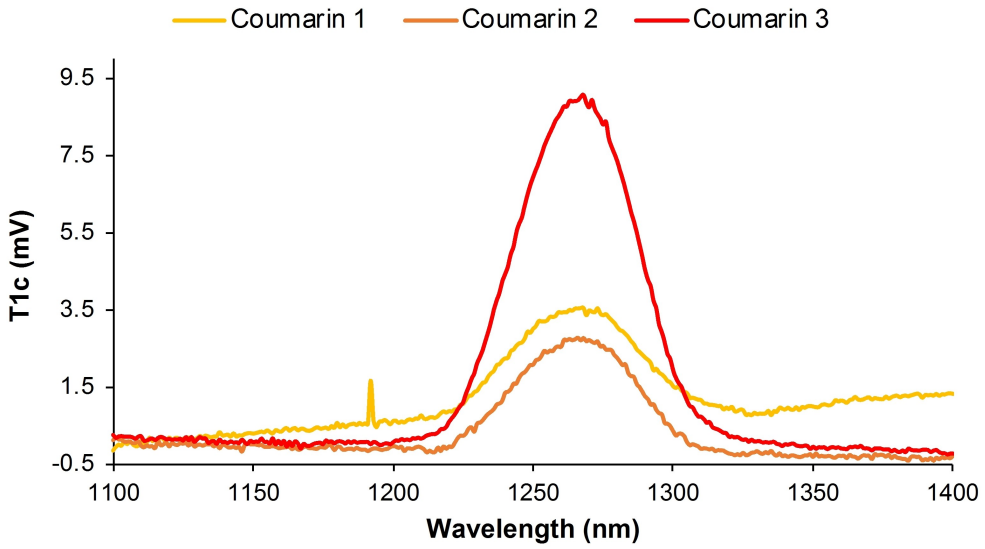

Figure 4. Singlet oxygen phosphorescence emission spectra (Ex at 405 nm) of 3-(*N*-methylpyridinium-4-yl)coumarins **1**–**3** in $CDCl_3$ (concentration: 5.0 μM), at 25 °C, recorded with a liquid nitrogen-cooled InGaAs single channel detector. See Supporting Information for parameters used to record spectra and for further phosphorescence emission spectra obtained upon 385 nm or 500 nm excitation.

one being further stabilized through an intramolecular hydrogen bond (Figure 3, bottom). Since *ortho*-formylation is an effective way to minimize the formation of non-fluorescent merocyanine-type form **11**, being prone to undergo ISC, production of singlet oxygen under illumination is very unlikely especially in aqueous buffers. However, in chlorinated solvent ($CHCl_3$ or $CDCl_3$), the ability of *ortho*-salicylaldehyde **3** to undergo deprotonation and to exist as the neutral form **11** is higher. Indeed, phosphorescence measurements of $^1O_2$ have clearly shown that this compound is a better type II photosensitizer[26] than its parent 7-hydroxycoumarin **2** in such non-polar solvent (Figure 4). This photophysical study was supplemented by measuring spectral properties of phenolic coumarins **2** and **3** in EtOH and $CHCl_3$ (Table 1 and see Supporting Information for the corresponding spectra). In EtOH, the equilibrium between the phenol and phenolate forms takes place as evidenced by the presence of two distinct bands in the corresponding absorption spectra (398/490 nm for **2** and 380/475 nm for **3**), whose respective magnitudes strongly depend on the concentration of coumarin solution. Consequently, it was not possible to determine molar extinction coefficients. By analogy with its spectral behavior in acetate buffer, only the phenol form of **2** was found to be emissive with a maximum centered at 476 nm. However, we failed to establish a linear relationship between its fluorescence emission (area under the curves) and absorption at the excitation wavelength used for recording emission spectra, required for the determination of relative fluorescence quantum yield. For *ortho*-formylated derivative **3**, the fluorescence spectrum is the sum of emission curves of phenol and phenolate forms centered at 470 nm and 535 nm respectively, with a predominance of the longer wavelength band possibly assigned to electronic structure **12**. In $CHCl_3$, the phenol form as the sole emissive species of **2** was unambiguously confirmed by the presence and position of absorption and emission bands centered at 405 nm and 477 nm respectively. Interestingly, in this chlorinated solvent, we also managed to observe spectral signature of non-fluorescent quinonoid form **9**, as a minor band centered at 545 nm and present in the corresponding absorption spectrum. A similar electronic absorption profile was obtained with coumarin **3** but the interpretation of its multi-band emission curve was not trivial. Indeed, we highlighted that this push-pull coumarin exhibited a significant red-edge effect,[27] as the result of dual interplaying photophysical processes namely excited-state intramolecular proton transfer (ESIPT) and ICT (see Supporting Information for a comprehensive characterization of red-edge phenomenon).[28]

In brief, this study confirms that the use of pyridinium-4-yl moiety as C3 coumarin substituent, is an effective way to red-shift absorption/emission maxima of 7-(diethylamino)/7-hydroxycoumarins but negatively impacts their fluorescence quantum yield by promoting non-radiative triplet loss mainly in aqueous media. However, the values of fluorescence brightness ($e\times\Phi_F$) remain satisfactory to consider the use of these long-wavelength fluorophores as signaling units in reaction-based sensing strategies (*vide infra*). More unusual, the ability of push-pull coumarins **1**–**3** to produce singlet oxygen upon photonic excitation, is particularly relevant in the perspective of the design of novel type II photosensitizers for mitochondria-based photodynamic therapy (PDT).[29] Indeed, the coumarin scaffold is scarcely considered in this context but, in addition to our observations, a recent contribution that describes a novel sulfur substitution strategy applied to this chromophore (*i.e.*, conversion of coumarins into thiocoumarins) may change the game.[30]

In situ formation of 7-(diethylamino)-3-(N-methylpyridinium-4-yl)coumarin from a phosphatase-responsive "covalent-assembly" fluorescent probe

In the field of activity-based sensing devoted to the monitoring of enzyme activities, one of the preferred approaches to devise high-performance small-molecule fluorescent probes relies on the incorporation of the suitable recognition moiety into aniline- or phenol-based fluorophores.[31] Indeed, the capping of an optically tunable amino or hydroxyl group by an enzyme-responsive trigger unit[32] enables to achieve modulation of fluorescence properties.[33] Upon enzymatic activation, a valuable intensometric "OFF-ON" response is often obtained. Within this context, we have originally studied the conversion of 7-hydroxy-3-(*N*-methylpyridinium-4-yl)coumarins **2** and **3** into fluorogenic enzyme substrates (notably for esterase detection, Scheme 2 top). However, our preliminary investigations have highlighted the lack of reactivity of 7-OH group of such compounds towards electrophilic acylating or alkylating agents (*e.g.*, acid anhydride or benzyl bromide derived from *O*-protected *para*-hydroxybenzyl alcohol (PHBA)), in line with the predominance of the quinonoid form favored by the strong electron-withdrawing effect of *N*-methylpyridinium-4-yl moiety. In order to overcome this bottleneck, we next explored the reactivity of non-cationic 8-formyl-7-hydroxy-3-(pyridin-4-yl)coumarin **13**; we managed to achieve its *O*-acetylation by treatment with acetic anhydride (Ac_2O), but subsequent *N*-methylation of the pyridin-4-yl group of **14** (MeI, TEA in MeCN at 50 °C) led to complete deprotection of the phenol, yielding 8-formyl-7-hydroxy-3-(pyridinium-4-yl)coumarin **3** (Scheme 2, bottom). These experimental results clearly show that 7-hydroxy-3-(pyridinium-4-yl)coumarin derivatives are not suitable for the design of enzyme-activated fluorogenic probes based on the conventional caging strategy applied to fluorescent phenols. As an alternative, we chose to assess the potential of *N*,*N*-diethylaniline counterpart **1** in activity-based fluorescence sensing of enzymes. Since this dialkylamino-coumarin derivative does not possess fluorogenic properties, the preferred strategy to construct related activatable fluorescent probes is to use the "covalent-assembly" principle.[34] This approach was pioneered by the Swager (2003) and Anslyn (2005) groups for the detection of fluoride ions and heavy metal cations (Cd(II), Ni(II) and Co(II)) respectively, through *in situ* formation of fluorescent 7-(diethylamino)coumarins (DEACs) from uncyclized precursors and triggered by the targeted analytes to be detected.[14,35] Its current popularity is well illustrated by dozens of publications disclosing various caged precursors of coumarins freely usable in various contexts (in vitro, *in cellulo* or *in vivo* animal models) for (bio)sensing, biomaging and small-molecule-based theranostic applications.[36,37,38] By analogy with enzyme-responsive coumarin-based "covalent-assembly" fluorescent probes previously developed in our group,[39] we have designed 2-hydroxycinnamonitrile derivative **17** whose the phenol moiety is masked with a phosphatase-labile PHBA-derived self-immolative spacer[40] (Scheme 3). Indeed, upon the action of targeted enzyme, the released phenolate readily reacts with the

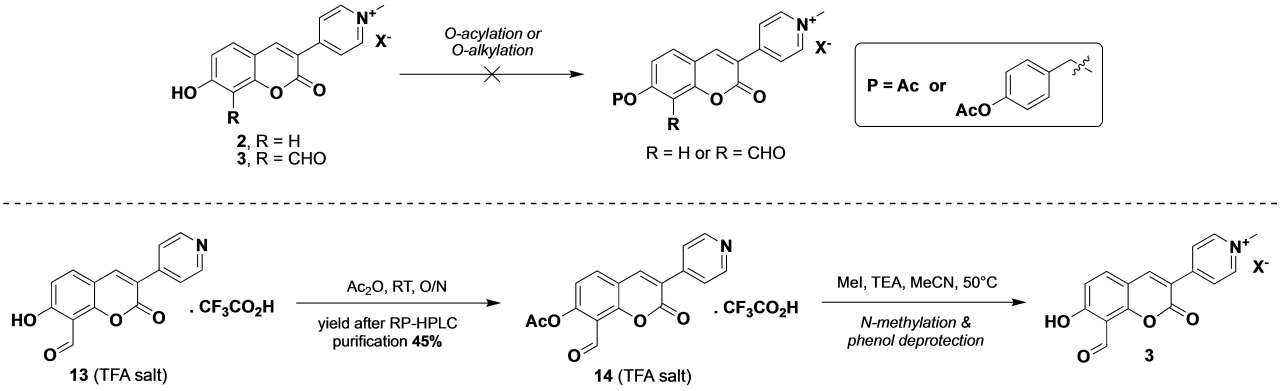

Scheme 2. (Top) Synthetic attempts towards esterase-responsive fluorescent probes based on phenol protection-deprotection of 3-(*N*-methylpyridinium-4-yl)coumarins **2** and **3**; (bottom) failed synthesis of esterase-sensitive fluorescent probe derived from 8-formyl-7-hydroxycoumarin **3**. [Ac = acetyl, Ac_2O = acetic anhydride, O/N = overnight, RT = room temperature, TEA = triethylamine, TFA = trifluoroacetic acid, X^- = iodide or trifluoroacetate anion].

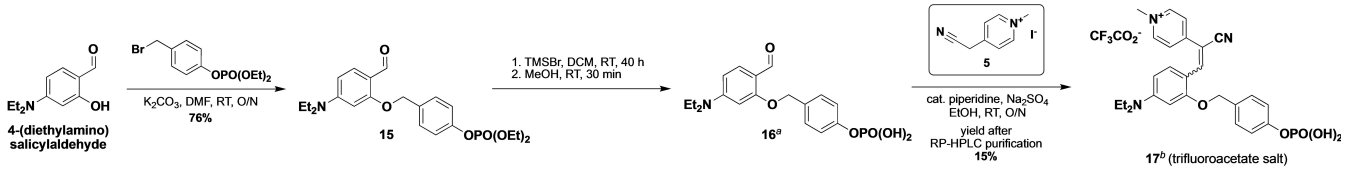

Scheme 3. Synthesis of ALP-responsive "covalent-assembly" fluorescent probe **17**. [cat. = catalytic amount, O/N = overnight, RT = room temperature, TMSBr = trimethylsilyl bromide]. [a] After drying under vacuum, this compound was directly used in the next step without purification (yield was assumed to be quantitative). [b] Please note: possible mixture of E and Z isomers are not differentiated by NMR and RP-HPLC analyses. We assumed that Z isomer is the major compound because during RP-HPLC-MS analyses of enzymatic reaction mixture (see with ALP Figure S9), we managed to detect only a minor amount of E isomer of dephosphorylated form of **17**, which is not able to undergo a rapid Pinner cyclization (contrary to Z isomer) to give 2-iminocoumarin **4**.

neighboring nitrile functional group (Pinner cyclization) to form 2-iminocoumarin intermediate **4** which slowly hydrolyzes to 7-(diethylamino)-3-(pyridinium-4-yl)coumarin **1** (Figures 1 and 6). We have chosen ALP as enzyme model to trigger *in situ* formation of this latter cationic coumarin. In addition to its popularity as a relevant blood biomarker for diagnosis of liver disease and certain bone disorders,[41] this enzyme has several positive attributes that will greatly facilitate the validation of the probe **17**: (1) a well-proven recognition moiety namely 4-phosphoryloxybenzyl,[42] (2) stability and full-compatibility with simple operating conditions (*i.e.*, Tris.HCl buffer, pH >8.0, 37 °C) and a commercial availability at a reasonable cost (especially for ALP from calf intestin). As shown in Scheme 3, the three-step synthetic sequence towards ALP-responsive probe **17** began with a Williamson-type etherification between commercial 4-(diethylamino)salicylaldehyde and diethyl 4-(bromomethyl)-phenylphosphonate performed under optimized conditions recently reported by us. Next, the conversion of diethyl phosphate derivative **15** to the corresponding acid **16** was achieved by prolonged treatment with an excess of TMSBr (5 equiv.) in dry DCM at room temperature. Final condensation of **16** with latent *C*-nucleophile 2-(*N*-methylpyridinium-4-yl)acetonitrile **5** was conducted in dry EtOH (containing anhydrous Na_2SO_4) at room temperature and promoted by piperidine-catalysis. The resulting

ALP-responsive "covalent-assembly" fluorescent probe **17** was isolated in a pure form by semi-preparative RP-HPLC (recovered as a TFA salt, overall yield for two steps 15%, based on TFA mass = 16.31% (0.85 molecule)). Having confirmed its structure by NMR (^{1}H, ^{13}C, ^{19}F and ^{31}P) and ESI-LRMS spectroscopic analyses (see Supporting Information), spectral features were examined in Tris.HCl buffer (10 mM, pH 8.0), the preferred medium for conducting ALP assays. Strong ICT character of **17** operating from the *N*,*N*-diethylamino donor group to the (*N*-methylpyridinium-4-yl)-substituted cyanomethylidenyl acceptor fragment, is illustrated by an intense and broad absorption band centered at 519 nm ($\varepsilon = 61\ 500\ M^{-1}cm^{-1}$, full-width half maximum, $\Delta\lambda_{1/2max} = 70$ nm). Excitation at 500 nm leads to a large Stokes-shifted ICT emission centered at 572 nm but the very low intensity prevented the determination of a fluorescence quantum yield. We then assumed that this fluorogenic enzyme substrate has the main positive feature of "covalent-assembly" fluorescent probes namely zero-background signal.[34] Our first *in vitro* enzyme assay was conducted with a 1.0 μM solution of probe **17** in Tris.HCl buffer (10 mM, pH 8.0) in the presence of ALP (10 U), using the set Ex/Em parameters (Ex/Em 470/550 nm) well suited for detecting coumarin **1**. As shown in Figure S1, a fast kinetics of activation (for both processes namely phosphate hydrolysis by ALP and Pinner cyclization) was obtained but fluorescence emission signal reached a low-intensity pseudo-plateau within 3 min. A prolonged incubation of this crude enzymatic mixture at 37 °C revealed a slow but steady increase of fluorescence emission at 550 nm within several hours, supporting the gradual hydrolysis of 2-iminocoumarin to **1** in aqueous Tris.HCl buffer. These results suggest that spectral features of 2-imino counterpart are dramatically different than those initially chosen for such time-course fluorescence measurements. In order to confirm this, we repeated this kinetics by stemming it after a short time. Fluorescence excitation/emission spectra were then recorded and maxima at 400/515 nm were found. Knowing this, further ALP assays and blank/control experiments were achieved using the two sets of detection parameters in a sequential manner (*i.e.*, Ex/Em 400/515 nm for 34 min then Ex/Em 470/550 nm for 4 h). After rapidly reaching the plateau indicating the complete conversion of **17** into **4** (Figure 6), a slight decrease of fluorescence emission at 515 nm was observed and interpreted as the slow hydrolysis of 2-iminocoumarin into coumarin **1** (Figure 5A and Figure 6). This latter one being poorly emissive at this wavelength (see Table 1 and Figure 2A). Conversely, when fluorescence parameters were tuned to optimal detection of this compound, a moderate but steady increase of fluorescence emission at 550 nm was observed (Figure 2B). Once the kinetics was stopped, the recording of emission curve revealed a remarkable 47-fold fluorescence increase (Figure 5C). Blank experiments also confirmed the full stability of the "covalent-assembly" fluorescent probe **17**. *In situ* formation of both 2-iminocoumarin **4** and final coumarin **1** was further demonstrated by RP-HPLC analyses of crude enzymatic mixtures either through fluorescence or ESI-MS detection, and conducted according to a well-established and reliable methodology developed by us (see Figure 7 for selected RP-HPLC-fluorescence elution profiles and Figures S2–S12 for all RP-HPLC-fluorescence and RP-HPLC-MS analyses). Whatever the kinetics analyzed (except for blank experiment that clearly illustrates the aqueous stability of "covalent-assembly" probe **17**, Figures 7E and 7F), a single and intense peak at $t_R = 3.6$ min assigned to 7-(diethylamino)-3-(*N*-methylpyridinium-4-yl)coumarin **1** was observed on the detection channel Ex/Em 470/550 nm (Figure 7B). Conversely, two low intensity peaks at $t_R = 2.4$ and 3.6 min were detected on the channel Ex/Em 400/515 nm dedicated to preferred visualization of 2-iminocoumarin intermediate **4** (*i.e.*, peak at $t_R = 2.4$ min), at least under neutral conditions. In order to optimize detection of this Pinner cyclization product under acidic RP-HPLC elution conditions (*i.e.*, ultrapure water and MeCN containing 0.1% FA), we also used a third channel Ex/Em 470/515 nm and a slight increase in the relative proportion between peaks at $t_R = 2.4$ min and $t_R = 3.6$ min was observed (Figure 7A). All these results suggest that the fluorescence quantum yield of the imino product is very low (*i.e.*, dramatically lower than the 1.5% value determined for **1** in Tris.HCl buffer, *vide supra*). As conclusion, despite a modest fluorescence brightness in buffered neutral conditions, 7-(diethylamino)-3-(*N*-methylpyridinium-4-yl)coumarin **1** was identified as an attractive photoactive molecular scaffold in the context of enzyme-responsive "covalent-assembly" probes that involves *in situ* formation of emissive 2*H*-1-benzopyran-2-one heterocyclic derivatives as signaling mechanism. Furthermore, the availability of *N*-methylpyridinium-4-yl moiety within its core structure should facilitate mitochondria targeting for both probing functions of this important cellular organelle and (photo)therapeutic applications.[43] As an example, ALP-responsive probe **17** may be a useful molecular diagnostics tool directed to hyperactive mitochondria in cancer cells, known for

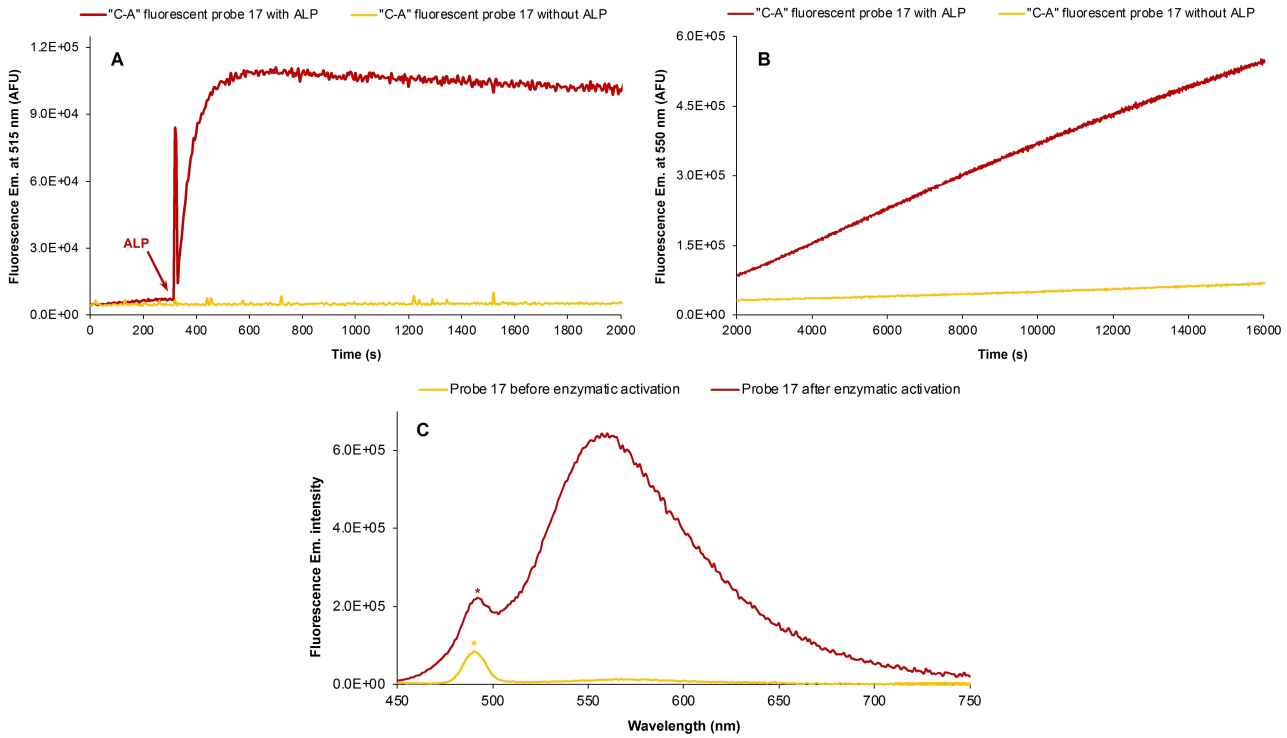

Figure 5. (A) Fluorescence emission time course (Ex/Em 400/515 nm, slits 5 nm) of ALP-responsive "covalent-assembly" fluorescent probe **17**, concentration: 1.0 μM, in the presence of ALP (10 U) in Tris.HCl buffer (10 mM, pH 8.0) at 37 °C. ALP was added after 5 min of incubation in Tris.HCl buffer alone. (B) Fluorescence emission time course (Ex/Em 470/550 nm, slits 5 nm) of the same solution incubated for a further 4 h at 37 °C. (C) Overlay of fluorescence emission spectra (Ex at 420 nm, slits 5 nm) of ALP-responsive "covalent-assembly" fluorescent probe **17** before and after incubation with ALP. Please note: peak marked with an asterix, at 490–492 nm is the Raman scattering peak of water. [ALP = alkaline phosphatase, "C–A" = "covalent-assembly"].

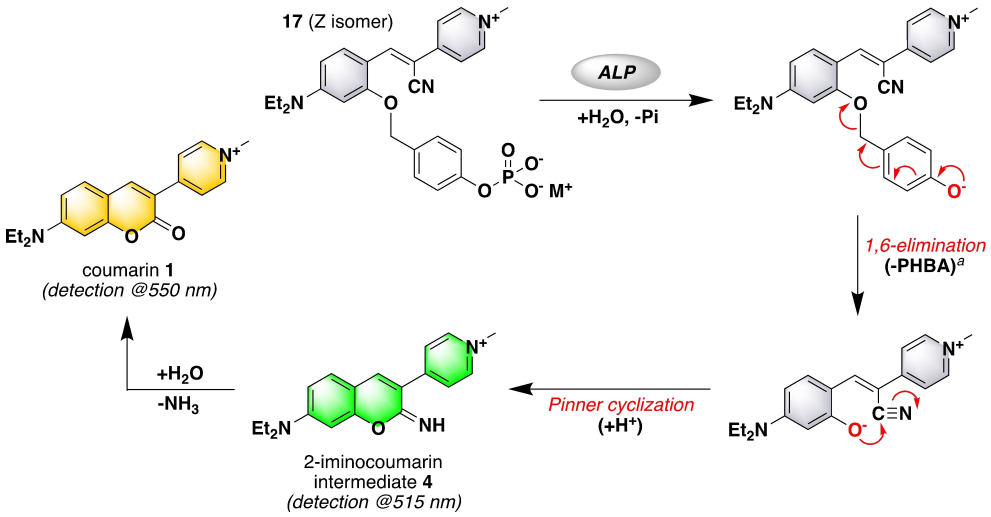

Figure 6. Detailed mechanism assumed for the activation of ALP-responsive "covalent-assembly" fluorescent probe **17**. Counter ion of pyridinium moiety is omitted for clarity. Only Z isomer of probe **17** that undergoes rapid Pinner cyclization is drawn. [a] Please note: 1,6-Elimination leads to the release of quinone methide that undergoes instantaneous hydration to give *para*-hydroxybenzyl alcohol (PHBA). [ALP = alkaline phosphatase, M^+ = cation not specified, Pi = phosphate ion].

their over-production of ATP and then characterized by an overexpression of this phosphatase.

Synthesis of an Fe(III)-salen complex based on ethylenediamine and 8-formyl-7-hydroxy-3-(N-methylpyridinium-4-yl)coumarin

Contrary to analytes endowed with dynamic molecular reactivity, the fluorogenic detection of biological anions in aqueous

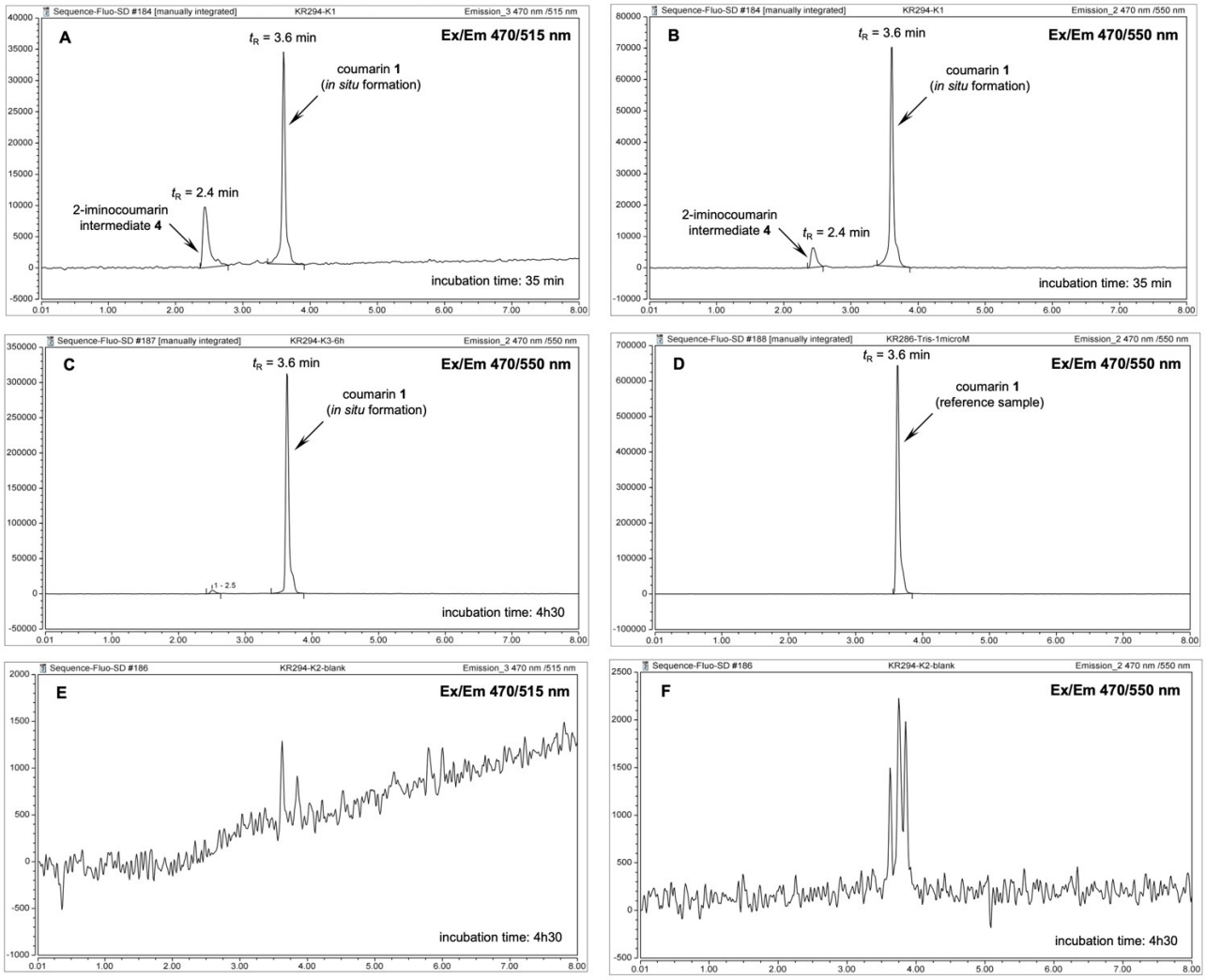

Figure 7. RP-HPLC elution profiles (system H, fluorescence detection Ex/Em 470/515 nm and 470/550 nm) of enzymatic reaction mixtures: (A–B) "covalent-assembly" fluorescent probe **17** with ALP (after 35 min of incubation), (C) covalent-assembly" fluorescent probe **17** with ALP (after 4 h30 of incubation), (D) 7-(diethylamino)-3-(*N*-methylpyridinium-4-yl)coumarin **1** (1.0 μM in Tris.HCl buffer), (E–F) "covalent-assembly" fluorescent probe **17** without ALP (blank, after 4 h30 of incubation).

environments, especially those chemically inert, remains an important challenge to be addressed. This is particularly the case with phosphate (Pi) and pyrophosphate (PPi) anions.[44] Indeed, real-time and/or accurate monitoring/quantification of such species is particularly important and implemented in various fields: (1) bioanalysis of nucleic acids (*e.g.*, real-time DNA sequencing, PCR, …), (2) disease diagnostics (*e.g.*, hypophosphatemia, calcium pyrophosphate dihydrate crystal deposition disease (CPPD), …), and (3) *in vitro* enzyme assays for biotechnology and diagnostics. Within this context, the Zelder group has recently proposed a valuable strategy for the selective detection of unreactive PPi anion based on the molecular disassembly of metal-salen complexes releasing water-soluble blue-cyan or green emissive *ortho*-salicylaldehyde derivatives (see Figure 1 for the simplified principle of PPi sensing strategy proposed by the Zelder group and virtually applied to coumarin **3**).[13,45,46] Among the most suited metal cations to obtain the best compromise between aqueous stability, selectivity for PPi anion and fine control of fluorescence properties (*i.e.*, quenching or shift in excitation/emission maxima) of the "molecular disassembly" probe, Fe(III) and Al(III) species were identified as the best candidates to provide an optimal "OFF-ON" fluorescence response and a ratiometric fluorescence output respectively. In order to expand this unusual activity-based sensing method to brightner salicylaldehyde signaling units, we have recently explored the use of *ortho*-formylated phenol-based fluorophores such as 8-formyl-7-hydroxycoumarin.[47] However, lukewarm results were obtained due to the low fluorescence quantum yield of this salicylaldehyde-containing fluorophore as compared to the quantum yield of parent 7-hydroxycoumarin (*i.e.*, 4% vs. 84% in HEPES buffer, pH 7.3). In the present case, since we have shown that *ortho*-formylation of 7-hydroxy-3-(*N*-methylpyridinium-4-yl)coumarin led to an increase of this photophysical parameters compared to parent phenol **2**, we contemplated the synthesis of the corresponding Fe(III)-salen complex derived from 1,2-

ethylenediamine (Scheme 4). One-pot formation of salen ligand and its subsequent metalation with anhydrous $FeCl_3$ were achieved using the following conditions: TFA salt of **3** was dissolved in dry EtOH-DMF (2:1 mixture, v/v), neutralized by adding an excess of DIEA, then added to solid $FeCl_3$, and finally mixed with 1,2-ethylenediamine (1 equiv.). The main challenge associated with this synthesis is related to the isolation of the newly formed acid-sensitive and highly polar metal complex. Semi-preparative RP-HPLC using volatile triethylammonium bicarbonate (TEAB, 50 mM, pH 7.0) buffer and MeCN as the mobile phase followed by freeze-drying (procedure repeated thrice to remove excess of TEAB), succeeded to isolate probe **18** in a pure form and with a satisfying yield of 52%. Its structure was confirmed by ESI-LRMS (both in the positive and negative mode, Figures 8A and 8B respectively) and UV-visible analyses. It should be pointed out in particular the presence of a broad and flat absorption band centered at ca. 570 nm assigned to a ligand-to-metal-charge-transfer (LMCT) band (Figure S13). Unfortunately, Fe(III)-salen complex **18** was found to be completely unstable in HEPES buffer (20 mM, pH 7.5), the preferred aqueous medium to perform fluorescence pyrophosphate assays. The complex was rapidly hydrolyzed to give back the parent 8-formyl-7-hydroxycoumarin **3**, especially at a relevant working concentration of 1.0 μM. Further confirmation of this poor aqueous stability was provided by preliminary *in vitro* PPi assays yielding unsatisfactory results (see Supporting Information). Indeed, before addition of analyte, background fluorescence of **18** was very high and no significant change in

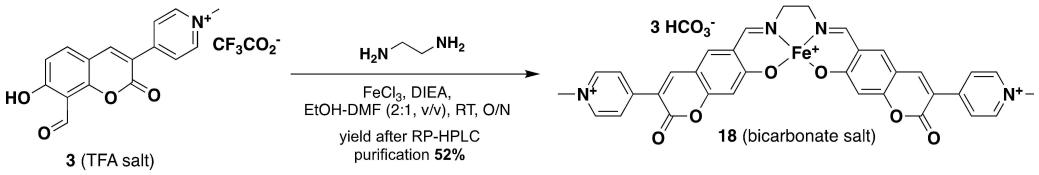

Scheme 4. Synthesis of coumarin-salen Fe(III) complex **18**. [DIEA = *N*,*N*-diisopropylethylamine, O/N = overnight, RT = room temperature].

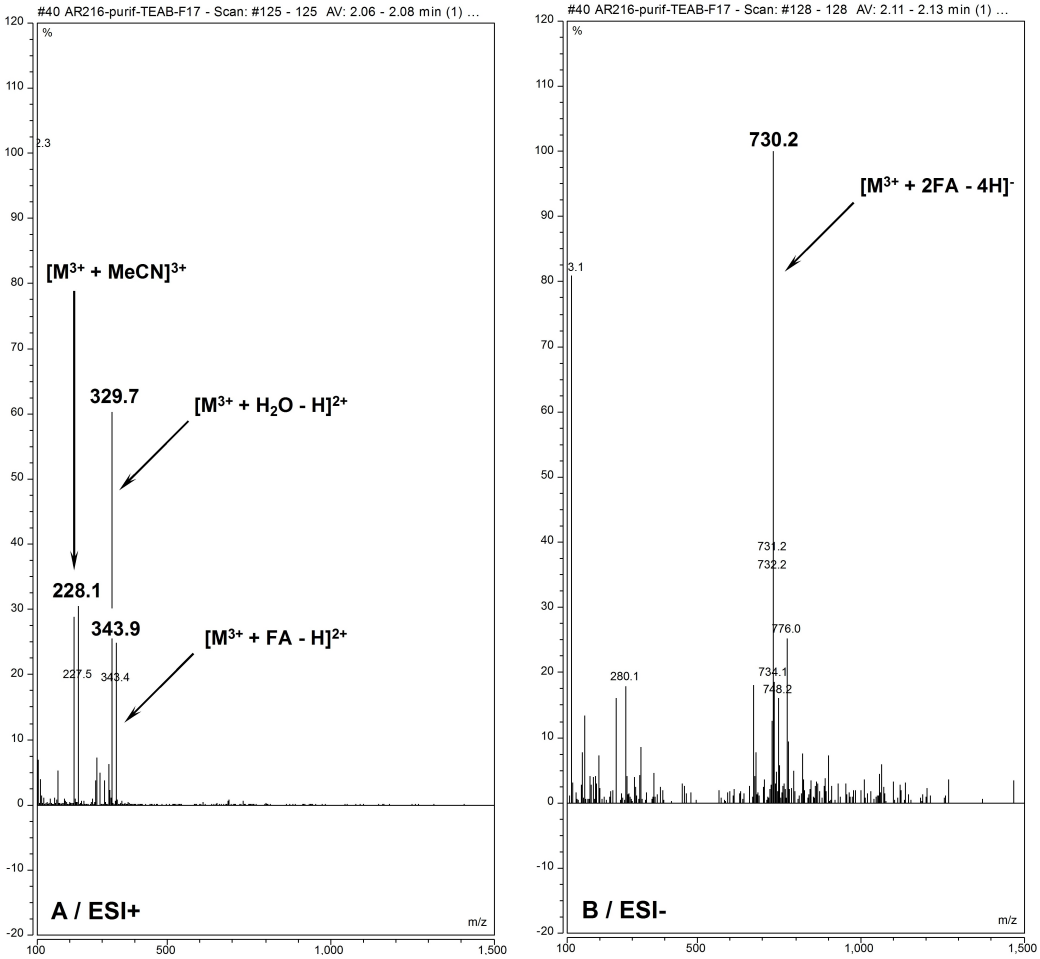

Figure 8. ESI mass spectra of coumarin-salen Fe(III) complex **18** recorded during RP-HPLC analysis (system A): (A) positive mode; (B) negative mode. [FA = formic acid].

signal intensity was observed upon addition of PPi anion (Figures S14–S15), thus supporting the lack of fluorogenic metal complex **18** in HEPES buffer solution. We hypothesized that the two *N*-methylpyridinium EWGs dramatically enhance the electrophilic reactivity of imine bridge and thus promotes demetalation and release of fluorescent *ortho*-salicylaldehyde-bearing coumarin **3**. In order to address this stability issue, we have also explored the synthesis of Fe(III)-salen complex derived from neutral 8-formyl-7-hydroxy-3-(pyridin-4-yl)coumarin **13** under the same previously described conditions. The formation of compound **19** was confirmed by RP-HPLC-MS analyses of the crude reaction mixture but we failed to isolate it by semi-preparative RP-HPLC. Only starting coumarin **13** was recovered in an almost quantitative manner, once again illustrating the too good leaving group character of 7-hydroxycoumarins bearing both C8-formyl and C3-pyridin-4-yl (free base or *N*-methylpyridinium form) groups, in the context of such metalated salen architectures.

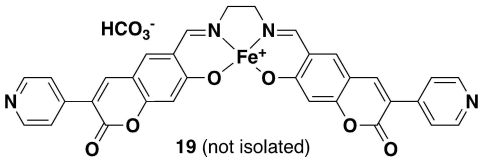

19 (not isolated)

This study clearly shows that 8-formyl-7-hydroxy-3-(*N*-methylpyridinium-4-yl)coumarin **3** cannot be used as a salicylaldehyde-based fluorescent reporter in the context of PPi-responsive "molecular disassembly" probes. Outside the field of molecular biosensing, since Fe(III)-salen complex **18** exhibits a dramatically higher stability in organic solvents (*e.g.*, $CHCl_3$, DMSO, …), the ability of related compounds to be used as a visible light photosensitizers for applications in photoredox catalysis would be worth assessing.[48]

Conclusions

In summary, we devised a simple and effective synthetic route towards 7-(diethylamino)- and 7-hydroxy-3-(*N*-methylpyridinium-4-yl)coumarins using latent *C*-nucleophile 2-(*N*-methylpyridinium-4-yl)acetonitrile **5** as key reactant. A comprehensive photophysical study of these two cationic coumarin fluorophores revealed some interesting features. The first one is the lack of fluorescence properties for 7-hydroxycoumarin derivative **2** in simulated physiological conditions (PB, 100 mM, pH 7.4) which was attributed to the large predominance of its neutral quinonoid form **11** in aqueous solution; this latter neutral compound undergoing ISC to T_1 excited state followed by partial energy transfer to molecular oxygen. The second one is the recovery of modest but real blue-green emissive properties attributed to the cationic phenol form in aqueous acidic conditions (acetate buffer, pH 4.3), thus suggesting that such push-pull structure may be further used for designing mitochondria-targeted pH-responsive fluorescent bioprobes.[49] In order to minimize the predominance of the non-fluorescent merocyanine form at physiological pH, we found that *ortho*-formylation functionalization of 7-hydroxycoumarin **2** is an effective way to achieve this by disrupting extended electronic delocalization from phenolate group to *N*-methylpyridinium moiety through a formal intramolecular proton transfer. Unfortunately, we have failed to exploit this valuable spectral characteristic in the context of Fe(III)-salen complexes as fluorogenic "OFF-ON" probes for selective detection of PPi anions. Indeed, even if we managed to synthesize and isolate metalated salen derivative **18** in a pure form, its poor aqueous stability was crippling for practical sensing applications in buffers or in biologicial media. Conversely, positive results obtained with the ALP-responsive "covalent-assembly" fluorescent probe **17** open interesting perspectives. Indeed, the use of latent *C*-nucleophiles related to 2-(*N*-methylpyridinium-4-yl)acetonitrile **5** in the Knoevenagel condensation step offers the unique opportunity to achieve facile late-stage functionalization of analyte-responsive caged precursors of coumarins[50] and pyronins[51] simply by changing the substituent used for pyridine *N*-quaternarization. This will enable to tune their physico-chemical properties (especially water solubility), targeting ability, pharmacokinetics (*e.g.*, introduction of a PEG linker) or to confer them release capabilities of a molecule of interest (*e.g.*, a drug or a second reporter). Furthermore, pyridine *N*-quaternarization may be used to achieve covalent immobilization of such probes over functionalized solid surfaces aimed at creating "smart" material sensors.[37b,c,52] This will undoubtedly contribute to the popularization of "covalent-assembly" strategy in the fields of biosensing, bioimaging and (photo)theranostics based on the use of "smart" photoactive organic molecules. Lastly, we aim to take advantage of the high affinity of *N*-alkylpyridinium derivatives for CB[n] hosts[53] in order to create supramolecular assemblies that are expected to also enhance performances of pyridinium-containing coumarin/pyronin "covalent-assembly" fluorescent probes in aqueous environments.[54] Such strategy is currently explored by us and will be reported in due course.

Experimental Section

General

Unless otherwise noted, all commercially available reagents and solvents were used without further purification. TLC was carried out on Merck Millipore or Supelco® DC Kieselgel 60 F-254 aluminum sheets (Merck group). The spots were directly visualized or through illumination with a UV lamp ($\lambda = 254/365$ nm). HPLC-grade MeCN was dried over alumina cartridges immediately prior to use (water content: 75 ppm determined by Karl Fischer titration), using a solvent purification system PureSolv PS-MD-5 model from Innovative Technology. Absolute EtOH ($\geq 99.7\%$, HiPerSolv CHROMANORM®, VWR) was dried by stirring over anhydrous Na_2SO_4 under Ar atmosphere immediately prior to use. DMF was purchased from Fisher Chemical ($> 99\%$, lab reagent grade), dried by storage over activated 3 Å molecular sieves and kept under Ar atmosphere. Triethylamine (TEA) was dried by distillation over KOH and stored over KOH pellets and kept under Ar atmosphere. HPLC-gradient grade acetonitrile (MeCN) was obtained from Fisher Chemical. All aqueous buffers used in this work and aqueous mobile-phases for RP-HPLC were prepared using water purified either with a PURELAB Ultra system or a Chorus PURELAB system (ELGA, VEOLIA, purified

to 18.2 MΩ.cm). Stock solutions of triethylammonium acetate (TEAA, 2.0 mM) and triethylammonium bicarbonate (TEAB, 1.0 mM) buffers were prepared from distilled TEA and glacial acetic acid or CO_2 gas, respectively. 4-(Diethylamino)salicylaldehyde was recrystallized in deionized water and dried by lyophilization, prior to use. 4-(Diethylamino)-2-[[4-(phosphonooxy)phenyl]-methoxy]benzaldehyde **16** [2921806-96-2] was prepared according to literature procedures.[42]

Instruments and Methods

Freeze-drying operations were performed either with a Christ Alpha 2–4 LD plus or a FreeZone (2.5-Liter) benchtop Labconco apparatus. Centrifugation steps were performed with a Sprout® Plus Mini Centrifuge instrument (Heathrow Scientific). ^{1}H-, ^{13}C-, ^{19}F- and ^{31}P-NMR spectra were recorded either on a Bruker Avance Neo 500 MHz (equipped with a 5 mm BBOF iProbe) or on a Bruker Avance III HD 600 MHz spectrometer (equipped with a 5 mm BBOF CryoProbe Prodigy). NMR spectroscopy chemical shifts are quoted in parts per million (δ) relative to TMS (for ^{1}H, and ^{13}C), $CFCl_3$ (for ^{19}F) or aq. 85% H_3PO_4 (for ^{31}P). For ^{1}H and ^{13}C spectra, calibration was made by using residual signals of partially deuterated solvent summarized in 2010 by Fulmer *et al.*[55] For all other nuclei, SR value obtained after zero-calibration of the corresponding reference was applied. *J* values are expressed in Hz. IR spectra were recorded with a Bruker Alpha FT-IR spectrometer equipped with a universal ATR sampling accessory. The bond vibration frequencies are expressed in reciprocal centimeters (cm^{-1}). Before July 2022, RP-HPLC-MS analyses were performed on a Thermo-Dionex Ultimate 3000 instrument (pump + autosampler at 20 °C + column oven at 25 °C) equipped with a diode array detector (Thermo-Dionex DAD 3000-RS) and MSQ Plus single quadrupole mass spectrometer. From July 2022, RP-HPLC-MS analyses were performed on a Thermo Scientific Vanquish™ Flex instrument (pump + autosampler at 20 °C + column oven at 25 °C) equipped with a UV-visible DAD and ISQ-EM single quadrupole mass spectrometer. For RP-HPLC analyses involving fluorescence detection, Thermo-Dionex Ultimate 3000 instrument was coupled to a RS fluorescence detector (Thermo-Dionex, FLD 3400-RS). Purifications by semi-preparative HPLC were performed on a Thermo-Dionex Ultimate 3000 instrument (semi-preparative pump HPG-3200BX) equipped with an RS Variable Detector (VWD-3400RS, four distinct wavelengths within the range 190–800 nm). Ion chromatography analyses (for the determination of TFA mass content in freeze-dried samples) were performed using a Thermo Scientific Dionex ICS 6000 ion chromatograph equipped with a conductivity detector CD (Thermo Scientific Dionex) and a conductivity suppressor ADRS 600 2 mm (Thermo Scientific Dionex), and according to a method developed by the PACSMUB staff.[56] Low-resolution mass spectra (LRMS) were recorded on a Thermo Scientific MSQ Plus single quadrupole instrument equipped with an electrospray (ESI) source. Elemental analyses were performed with a Thermo Scientific Flash Smart CHNS/O microanalyzer. See Supporting Information for all details related to instruments and methods for photophysical characterizations of 3-(*N*-methylpyridinium-4-yl)coumarins and related "covalent-assembly" fluorescent probe **17**.

High-Performance Liquid Chromatography Separations

Several chromatographic systems were used for the analytical experiments and the purification steps: System A: RP-HPLC-MS with Vanquish™ Flex instrument (Phenomenex Kinetex C_{18} column, 2.6 μm, 2.1×50 mm) with MeCN (+0.1% FA) and 0.1% aq. formic acid (aq. FA, pH 2.1) as eluents [5% to 100% (5 min) of MeCN, then 100% MeCN (3 min)] at a flow rate of 0.5 mL/min. UV-visible detection was achieved at 220, 260, 350 and 500 nm (+DAD 190–800 nm allowing extraction of any single wavelength channel within this spectral range). Low resolution ESI-MS detection (ISQ-EM detector) in the positive/negative mode with the following parameters: full scan, 100–1000 a.m.u., spectrum type: centroid, dwell or scan time: 1 s, source CID voltage: 20 V, vaporizer temperature: 282 °C, ion transfer tube temperature: 300 °C, source voltage positive ions: 3 kV, source voltage negative ions: 2 kV, sheet gas pressure: 49.9 psig (3.4 bars), aux gas pressure: 5.7 psig (0.35 bar) and sweep gas pressure: 0.5 psig (0.035 bar). System A′: system A with Thermo-Dionex Ultimate 3000 instrument (before July 2022). UV-visible detection was achieved at 220, 260, 450 and 500 nm (+DAD 220–700 nm allowing extraction of any single wavelength channel within this spectral range. Low resolution ESI-MS detection (MSQ Plus) in the positive/negative mode (full scan, 100–1000 a.m.u., data type: centroid, needle voltage: 3.0 kV, probe temperature: 350 °C, cone voltage: 75 V and scan time: 1 s. System B: semi-preparative RP-HPLC (SiliCycle SiliaChrom C_{18} column, 10 μm, 20×250 mm) with MeCN and aq. 0.1% TFA (pH 1.9) as eluents [0% MeCN (15 min), followed by a linear gradient from 0% to 100% MeCN (56 min)] at a flow rate of 20.0 mL/min. Quadruple UV-visible detection was achieved at 220, 260, 340 and 375 nm. System C: system B with the following gradient [0% MeCN (10 min), followed by a linear gradient from 0% to 100% MeCN (100 min)]. Quadruple UV-visible detection was achieved at 220, 260, 370 and 400 nm. System D: system B with quadruple UV-visible detection at 220, 260, 290 and 595 nm. System E: system B with the following gradient [10% MeCN (5 min), followed by a gradient from 10% to 30% (7.5 min), then 30% to 100% (70 min). Quadruple UV-visible detection at 220, 260, 480 and 520 nm. System F: system E with the following gradient [0% MeCN (5 min), followed by a gradient from 0% to 30% (12 min), then 30% to 100% (100 min). System G: system B with MeCN and aq. TEAB buffer (50 mM, pH 7.0–7.5) as eluents [0% MeCN (10 min), followed by a linear gradient from 0% to 75% (100 min)] at a flow rate of 20.0 mL/min. Quadruple UV-visible detection was achieved at 220, 260, 470 and 525 nm. System H: system A′ with fluorescence detection (at 45 °C) with the following sets of parameters: Ex/Em channels 400/515 nm, 470/515 nm and 470/550 nm (sensitivity: 1, PMT: pmt1, filter wheel: Auto). System I: system A with the following gradient [5% to 100% (5 min) of MeCN, then 100% MeCN (1.5 min)]. Low resolution ESI-MS detection (ISQ-EM detector) in the positive/negative mode with the following parameters: full scan, 100–1500 a.m.u.; SIM(+/−), *m/z* 494.2 ± 0.25 and 492.2 ± 0.25 for **17**; SIM(+), *m/z* = 308.2 ± 0.25 for **4**; SIM(+), *m/z* = 309.2 ± 0.25 for **1**.

Syntheses

*Please note: due to high polarity and water solubility of molecules bearing N-methylpyridinium moiety, intermediates in the multi-step synthesis of coumarins **2** and **3** (i.e., latent C-nucleophile **5** and 2-iminocoumarin derivatives) could not be not purified by liquid-liquid extraction or conventional column chromatography over SiO_2. Thus, they were used in the next steps as a mixture with triethylammonium chloride (TEA.HCl), the salt formed during the N-quaternization reaction of 2-(pyridin-4-yl)acetonitrile (ratio determined by ^{1}H NMR). Furthermore, isolation of 2-iminocoumarin derivatives by semi-preparative RP-HPLC (with aq. 0.1% FA or TFA, and MeCN as eluents) was not regarded due to their conversion into the corresponding coumarins through acid-mediated hydrolysis of their imine moiety, observed during our preliminary attempts of purifications.*

7-(Diethylamino)-3-(N-methylpyridinium-4-yl)coumarin, iodide 1 [2595405-93-7][6]

4-(Cyanomethyl)-1-methylpyridinium, iodide salt, (188 mg, 0.7 mmol, 1 equiv.) and recrystallized 4-(diethylamino)salicylaldehyde (140 mg, 0.72 mmol, 1 equiv.) were mixed and solubilized in dry EtOH (10 mL). Then, catalytic amount of piperidine (1 drop) was added and the resulting reaction mixture was stirred at RT overnight. The reaction was checked for completion by TLC (DCM/MeOH 85:15, v/v) and volatiles were under reduced pressure. Thereafter, aq. 1.0 M HCl was added (5 mL) and the resulting reaction mixture was heated under reflux for 1 h. After cooling to RT, the desired product progressively precipitated and the newly formed powder was filtered, washed with Et_2O and finally lyophilized. Iodide salt of 7-(diethylamino)-3-(*N*-methylpyridinium-4-yl)coumarin **1** was recovered as a red amorphous powder (105 mg, 0.2 mmol, yield 33%). IR (ATR): $\nu = 3376, 3114, 3078, 3021, 2967, 2926, 1693, 1637, 1615, 1574, 1505, 1456, 1414, 1369, 1348, 1337, 1319, 1308, 1285, 1271, 1239, 1197, 1135, 1090, 1074, 1040, 1018, 987, 962, 939, 855, 831, 796, 767, 712, 699, 637, 613$; ^{1}H NMR (500 MHz, [D$_6$]DMSO): $\delta = 8.87$ (d, $J = 7.1$ Hz, 2H), 8.85 (s, 1H), 8.53 (d, $J = 7.0$ Hz, 2H), 7.62 (d, $J = 9.0$ Hz, 1H), 6.87 (dd, $J = 9.1$ Hz, $J = 2.4$ Hz, 1H), 6.64 (d, $J = 2.4$ Hz, 1H), 4.27 (s, 3H), 3.52 (q, $J = 7.1$ Hz, 4H), 1.16 (t, $J = 7.0$ Hz, 6H); ^{13}C NMR (126 MHz, [D$_6$]DMSO) $\delta = 159.4, 157.4, 153.0, 150.7, 146.5, 144.4, 131.7, 123.4, 110.5, 110.0, 108.4, 96.0, 46.8, 44.5, 12.4$; HPLC (system A): $t_R = 3.2$ min (purity 99% at 260 nm and 99% at 475 nm); LRMS (ESI+, recorded during RP-HPLC analysis): *m/z* 309.2 [M]$^+$ (100), calcd for $C_{19}H_{21}N_2O_2^+$ 309.2; Elemental analysis calcd for $C_{19}H_{21}IN_2O_2$. 0.5 NH_4Cl: C 49.29, H 5.01, N 7.56, O 6.91; found: C 49.39, H: 4.98, N 6.74, O 7.91; UV-vis (recorded during RP-HPLC analysis): $\lambda_{max} = 205$ nm, 253 nm, 475 nm; UV-vis (PB, pH 7.5, 25 °C): $\lambda_{max} = 475$ nm (ε 48 500 $M^{-1}cm^{-1}$); UV-vis (Tris.HCl buffer, pH 8.0, 25 °C): $\lambda_{max} = 475$ nm (ε 48 850 $M^{-1}cm^{-1}$); UV-vis (EtOH, 25 °C): $\lambda_{max} = 482$ nm (ε 49 300 $M^{-1}cm^{-1}$); UV-vis ($CHCl_3$, 25 °C): $\lambda_{max} = 500$ nm (ε 58 000 $M^{-1}cm^{-1}$); Fluorescence (PB, pH 7.5, 25 °C): $\lambda_{max} = 558$, $\Phi_F = 2\%$; Fluorescence (Tris.HCl buffer, pH 8.0, 25 °C): $\lambda_{max} = 558$ nm; Fluorescence (EtOH, 25 °C): $\lambda_{max} = 561$ nm, $\Phi_F = 27\%$, τ (nanoLED @ 495 nm) = 1.4 ns; Fluorescence ($CHCl_3$, 25 °C): $\lambda_{max} = 550$ nm, $\Phi_F = 25\%$, τ (nanoLED @ 495 nm) = 1.9 ns and 2.8 ns.

7-Hydroxy-3-(N-methylpyridinium-4-yl)coumarin, trifluoroacetate 2

(CAS [98805-48-2] for iodide salt)[6]

(a) N-alkylation: Commercial 2-(pyridin-4-yl)acetonitrile; hydrochloride salt (500 mg, 3.3 mmol, 1 equiv.) and dry TEA (0.544 mL, 3.9 mmol, 1.2 equiv.) were mixed and dissolved in dry MeCN (6 mL). Then, methyl iodide (1.4 mL, 22.7 mmol, 7 equiv.) was added and the resulting reaction mixture was heated at 50 °C for 1 h. The reaction was checked for completion by TLC (DCM/MeOH 85:15, v/v). After complete evaporation under reduced pressure, the resulting residue was triturated and washed with Et_2O to give a black powder identified as the iodide salt of 4-(cyanomethyl)-1-methylpyridinium [92384-22-0] (mixed with tritethylammonium chloride, TEA.HCl, 1:1 mixture). After drying under vacuum, this latent *C*-nucleophile was directly used in the next step without further purification.

(b) Knoevenagel condensation and Pinner cyclization: 4-(Cyanomethyl)-1-methylpyridinium, iodide salt, (3.3 mmol, 1 equiv.) and 2,4-dihydroxybenzaldehyde (449 mg, 3.3 mmol, 1 equiv.) were mixed and solubilized in dry EtOH (40 mL). Then, catalytic amount of piperidine (1 drop) was added and the resulting reaction mixture was stirred at RT overnight. The reaction was checked for completion by RP-HPLC-MS (system A, $t_R = 2{,}2$ min) and volatiles were removed under reduced pressure. Thereafter, Et_2O was added to precipitate the product. The resulting brown powder was washed with Et_2O and dry under vacuum to give iodide salt of 7-hydroxy-3-(*N*-methylpyridinium-4-yl)-2-iminocoumarin (mixed with TEA.HCl, 47:53 mixture, 1.54 g, yield (over two steps a-b) 89%). which was directly used in next steps without further purification.

(c) Acid hydrolysis of imine moiety: 2-Iminocoumarin (120 mg, 0.3 mmol, 1 equiv.) was dissolved in MeCN (25 mL). Then, aq. 4.0 M HCl was added (10 mL) and the resulting reaction mixture was heated at 50 °C for 2 h. The reaction was checked for completion by RP-HPLC-MS (system A, $t_R = 2.0$ min). Thereafter, the mixture was cooled to 0–4 °C with an ice-water bath, neutralized by adding aq. 50% (w/v) NaOH (5 mL) and finally evaporated under reduced pressure. The resulting residue was purified by semi-preparative RP-HPLC (system B, $t_R = 29.0$–32.0 min). The product containing fractions were lyophilized to give TFA salt of 7-hydroxy-3-(*N*-methylpyridinium-4-yl)coumarin **2** as a yellow amorphous powder (76 mg, 0.2 mmol, yield 57% based on TFA mass = 39.5% determined by ion chromatography). IR (ATR): $\nu = 3066, 2453, 1702, 1670, 1647, 1611, 1564, 1524, 1502, 1468, 1415, 1373, 1340, 1305, 1233, 1197, 1169, 1133, 943, 846, 826, 799, 768, 738, 718, 638, 622$; ^{1}H NMR (500 MHz, [D$_6$]DMSO): $\delta = 11.37$ (s, 1H, O*H*), 8.98 (d, $J = 6.6$ Hz, 2H), 8.86 (s, 1H), 8.52 (d, $J = 6.5$ Hz, 2H), 7.72 (d, $J = 8.6$ Hz, 1H), 6.93 (dd, $J = 8.5$, 2.3 Hz, 1H), 6.84 (d, $J = 2.2$ Hz, 1H), 4.32 (s, 3H); ^{13}C NMR (126 MHz, [D$_6$]DMSO): $\delta = 164.2, 158.9, 156.4, 150.3, 146.8, 144.9, 131.8, 124.9, 115.3, 114.5, 111.5, 102.0, 47.2$; ^{19}F NMR (470 MHz, [D$_6$]DMSO): $\delta = -73.6$ (s, 3F, C*F*$_3$-TFA); HPLC (system A): $t_R = 2.0$ min (purity 99% at 260 nm and 99% at 375 nm); LRMS (ESI+, recorded during RP-HPLC analysis): *m/z* 254.1 [M]$^+$ (100), calcd for $C_{15}H_{12}NO_3^+$ 254.1; UV-vis (recorded during RP-HPLC analysis): $\lambda_{max} = 197$ nm, 248 nm, 375 nm; UV-vis (PB, pH 7.4, 25 °C): $\lambda_{max} = 447$ nm (ε 39 950 $M^{-1}cm^{-1}$); UV-vis (NaOAc buffer, pH 4.3, 25 °C): $\lambda_{max} = 379$ nm (ε 31 400 $M^{-1}cm^{-1}$); Fluorescence (NaOAc buffer, pH 4.3, 25 °C): $\lambda_{max} = 467$ nm, $\Phi_F = 1\%$.

8-Formyl-7-hydroxy-3-(N-methylpyridinium-4-yl)coumarin, trifluoroacetate 3

To a solution of 7-hydroxy-2-iminocoumarin derivative **2** (773 mg, 1.6 mmol, 1 equiv.) in TFA (16 mL), hexamine (524 mg, 3.7 mmol, 2.3 equiv.) was added and the resulting reaction mixture was heated under reflux for 9 h. The reaction was checked for completion by RP-HPLC-MS (system A, $t_R = 2.2$ min). After cooling to 0–4 °C with an ice-water bath, aq. 4.0 M HCl (15 mL) was added and the mixture was stirred for further 45 min. Thereafter, the mixture was evaporated under reduced pressure and the resulting residue was directly purified by semi-preparative RP-HPLC (system C, $t_R =$ 35.0–38.0 min). The product containing fractions were lyophilized to give TFA salt of 8-formyl-7-hydroxy-3-(*N*-methylpyridinium-4-yl)coumarin **3** as an orange powder (123 mg, 0.2 mmol, yield 14% based on TFA mass = 48.0% determined by ion chromatography). IR (ATR): $\nu = 3066, 2545, 1714, 1669, 1644, 1598, 1564, 1522, 1456, 1408, 1338, 1308, 1235, 1192, 1160, 1120, 1063, 951, 847, 816, 794, 771, 716, 650, 618$; ^{1}H NMR (500 MHz, [D$_6$]DMSO): $\delta = 12.52$ (s, 1H, O*H*), 10.47 (s, 1H, C*H*O), 9.02 (d, $J = 6.7$ Hz, 2H), 8.90 (s, 1H), 8.52 (d, $J = 6.9$ Hz, 2H), 7.98 (d, $J = 8.8$ Hz, 1H), 7.11 (d, $J = 8.8$ Hz, 1H), 4.34 (s, 3H);^{13}C NMR (126 MHz, [D$_6$]DMSO): $\delta = 189.2, 166.2, 158.0, 155.9, 149.8, 146.5, 145.2, 137.2, 125.1, 116.5, 115.2, 111.2, 109.6, 47.3$; ^{19}F NMR (470 MHz, [D$_6$]DMSO): $\delta = -73.9$ (s, 3F, C*F*$_3$-TFA); HPLC (system A): $t_R = 2.2$ min (purity 99% at 260 nm and 99% at 370 nm); LRMS (ESI+, recorded during RP-HPLC analysis): *m/z* 282.2 [M]$^+$ (100), calcd for $C_{16}H_{12}NO_4^+$ 282.1; UV-vis (recorded during RP-HPLC analysis): $\lambda_{max} = 193$ nm, 263 nm, 370 nm; UV-vis (PB, pH 7.5, 25 °C): $\lambda_{max} = 440$ nm (ε 57 800 $M^{-1}cm^{-1}$); UV-vis (DMSO, 25 °C): $\lambda_{max} = 378$ nm (ε 14 200 $M^{-1}cm^{-1}$) and 495 nm (ε 75 300 $M^{-1}cm^{-1}$). UV-vis

($CHCl_3$, 25 °C): λ_{max} = 386 nm (ε 39 950 $M^{-1}cm^{-1}$); Fluorescence (PB, pH 7.4, 25 °C): λ_{max} = 520 nm, Φ_F = 1 %; Fluorescence ($CHCl_3$, 25 °C): λ_{max} = 532 nm, τ (nanoLED @ 373 nm) = 0.95 ns (Em centered at 466 nm), τ (nanoLED @ 373 nm) = 0.9 ns (Em centered at 530 nm).

ALP-responsive coumarin caged precursor 17

4-(Cyanomethyl)-1-methylpyridinium, iodide salt (42 mg, 161 μmol, 1.1 equiv.) and benzaldehyde **16** (57 mg, 150 μmol, 1 equiv.) were mixed and dissolved in dry EtOH (5 mL). Then, anhydrous Na_2SO_4 (10 mg) and catalytic amount of piperidine (1 drop) were sequentially added and the resulting reaction mixture was stirred at RT overnight. The reaction was checked for completion by RP-HPLC-MS (system A', t_R = 4.0 min). The mixture was evaporated under reduced pressure and the resulting residue was directly purified by semi-preparative RP-HPLC (system E, t_R = 23.5–25.0 min). *Please note: optimization of gradient HPLC was achieved for the next purifications (system F, t_R = 30.5–32.0 min).* The product containing fractions were lyophilized to give TFA salt of ALP-responsive "covalent-assembly" fluorescent probe **17** as a red amorphous powder (13.5 mg, 23 μmol, yield 15 % based on TFA mass = 16.3 % determined by ion chromatography). IR (ATR): ν = 2974, 2362 (w), 2202 (w, CN), 1741 (w), 1688 (w), 1643, 1610, 1549, 1503, 1410, 1339, 1318, 1268, 1216, 1184, 1118, 1073, 1015 (w), 922, 812, 789, 702, 684, 637, 624 ;^{1}H NMR (600 MHz, [D_6]DMSO): δ = 8.74 (d, *J* = 7.2 Hz, 2H), 8.42 (s, 1H), 8.28 (d, *J* = 9.0 Hz, 1H), 7.95 (d, *J* = 7.2 Hz, 2H), 7.46 (d, *J* = 8.4 Hz, 2H), 7.18 (d, *J* = 7.8 Hz, 2H), 6.59 (dd, *J* = 9.6 Hz, *J* = 2.4 Hz, 1H), 6.31 (d, *J* = 2.4 Hz, 1H), 5.26 (s, 2H), 3.50 (q, J = 7.2 Hz, 4H, C*H*$_2$-Et), 1.13 (t, *J* = 7.2 Hz, 6H, C*H*$_3$-Et); ^{13}C NMR (151 MHz, [D_6]DMSO): δ = 161.4, 154.0, 151.1, 144.8, 143.0, 130.2, 128.7, 120.4, 120.1, 120.0, 118.3, 109.8, 106.3, 95.0, 92.7, 69.8, 46.4, 44.5, 12.6; ^{19}F NMR (564.6 MHz, [D_6]DMSO): δ = −73.4 (s, 3F, C*F*$_3$-TFA); ^{31}P NMR (243 MHz, [D_6]DMSO): δ = −5.43 (s, 1P, *P*-phosphate); HPLC (system A): t_R = 3.5 min (purity 100 % at 270 nm and > 99 % at 520 nm); LRMS (ESI+, recorded during RP-HPLC analysis): *m/z* 494.2 $[M]^+$ (100) and 987.4 $[2\ M^+–H]^+$ (25), calcd for $C_{26}H_{29}N_3O_5P^+$ 494.2; LRMS (ESI-, recorded during RP-HPLC analysis): *m/z* 492.2 $[M^+–2H]^-$ (100) and 985.5 $[2\ M^+–3H]^-$ (40), calcd for $C_{26}H_{27}N_3O_5P^-$ 492.2; UV-vis (recorded during RP-HPLC analysis): λ_{max} = 270, 288 and 521 nm; UV-vis (Tris.HCl buffer, pH 8.0, 25 °C): λ_{max} = 269 nm (ε 7 300 $M^{-1}cm^{-1}$), 288 nm (ε 6 700 $M^{-1}cm^{-1}$) and 519 nm (ε 61 500 $M^{-1}cm^{-1}$); Fluorescence (Tris.HCl buffer, pH 8.0, 25 °C): λ_{max} = 572 nm (too weak emission for an accurate determination of a relative fluorescence quantum yield).

Coumarin-salen Fe(III) complex 18

TFA salt of *ortho*-salicylaldehyde **3** (15.3 mg, 28.1 μmol, 2 equiv.) was dissolved in a mixture EtOH/DMF (2 : 1, v/v, 1.5 mL) and neutralized by adding DIEA (11.3 μL, 64.9 μmol, 4.6 equiv.). A rapid color change (from light yellow to intense orange) and precipitate formation were observed. Thereafter, this heterogeneous solution was added to a 10 mL round-bottom flask containing anhydrous $FeCl_3$ (3.75 mg, 23.1 μmol, 1.65 equiv.). The resulting mixture immediately became clear and turned to brown-kaki. Then, 1,2-ethylenediamine in solution in EtOH (10 μL of 1.4 M solution, 14 μmol, 1 equiv.) was added and the resulting reaction mixture was stirred at RT, protected from light, for 19 h. The reaction was checked for completion by RP-HPLC (system A), directly diluted with aq. TEAB buffer (50 mM, pH 7.0, 5 mL) and purified by semi-preparative RP-HPLC (system G, t_R = 50.0–58.5 min). The product containing fractions were lyophilized thrice to give the desired Fe(III)-salen complex as a brown amorphous powder (HCO_3^- salt, 6 mg, yield 52 % based on HCO_3^- mass = 22.2 %). *Please note: this compound must be lyophilized in the lack of other samples containing traces of FA or TFA to keep its integrity (i.e., to avoid demetalation and subsequent hydrolysis of salen ligand into parent 8-formyl-7-hydroxycoumarin **3**).* HPLC (system A): t_R = 2.1 min; LRMS (ESI+, recorded during RP-HPLC analysis): *m/z* 214.1 $[M^{3+}]^{3+}$ (30), 228.1 $[M^{3+} + MeCN]^{3+}$ (30), 329.7 $[M^{3+} + H_2O–H]^{2+}$ (60), 343.9 $[M^{3+} + FA–H]^{2+}$ (25), calcd for $C_{34}H_{26}FeN_4O_6^{3+}$ 642.1; LRMS (ESI-, recorded during RP-HPLC analysis): *m/z* 730.3 $[M^{3+} + 2FA–4H]^-$ (90), calcd for $C_{34}H_{22}FeN_4O_6^-$ 638.1; UV-vis (recorded during RP-HPLC analysis): λ_{max} = 271, 401 and 558 nm. UV-vis (DMSO, 25 °C): λ_{max} = 388 nm (ε 17 450 $M^{-1}cm^{-1}$), 488 nm (ε 35 200 $M^{-1}cm^{-1}$) and 570 nm (sh, ε 4 300 $M^{-1}cm^{-1}$). UV-vis ($CHCl_3$, 25 °C): λ_{max} = 386 nm (sh, ε 9 900 $M^{-1}cm^{-1}$), 476 nm (ε 17 500 $M^{-1}cm^{-1}$) and 535 nm (ε 22 700 $M^{-1}cm^{-1}$).

In vitro Activation of ALP-Responsive "Covalent-Assembly" Fluorescent Probe 17

Experimental details about stock solutions of fluorophore, probe, enzyme and buffer

- 1.0 mg/mL stock solutions of fluorophore **1** (2.3 mM) and ALP-responsive "covalent-assembly" fluorescent probe **17** (1.7 mM) were prepared in DMSO (UV-spectroscopy grade, Honeywell Riedel-de-Haën). *Please note: these solutions were stored at 4 °C (frozen DMSO) and found to be full-stable over several months.*
- Commercial ALP (from calf intestine, #P4978, 10 U/μL, storage buffer: 10 mM Tris.HCl (pH 8.2), 50 mM KCl, 1 mM $MgCl_2$, 0.1 mM $ZnCl_2$, 50 % glycerol, Sigma-Aldrich) was stored at −20 °C and directly used without dilution.
- Tris.HCl buffer (10 mM, pH 8.0) prepared in ultrapure H_2O.

Fluorescence-based bioassays

All assays were performed at 37 °C (using a Lauda Ecoline Recirculating Chiller RE 106 combined with a temperature controller Lauda E100, connected to the spectrofluorometer cell holder) and conducted with magnetic stirring. Probe's concentration in 3.5 mL fluorescence quartz cell was set to 1.0 μM. The volume of the probe's solution was always 3.0 mL. The following sets of detection parameters were used:

- Ex/Em 470/515, slits 5 nm, for the detection of *in situ* formed 2-iminocoumarin **4**,
- Ex/Em 470/550, slits 5 nm, for the detection of coumarin **1** formed through the slow hydrolysis of 2-iminocoumarin **4**.

Fluorescence emission of *in situ* formed (2-imino)coumarin was monitored at the suitable Ex/Em wavelength pair, over time with measurements every 5 s (duration of assay: 4 h30). 10 U (1.0 μL) of ALP was added after 5 min of incubation in buffer alone. Blank experiments to assess the stability of the "covalent-assembly" probes in Tris.HCl buffer, were achieved in the same way but without adding ALP. For each kinetics, fluorescence emission spectrum of the probe **17** was recorded before and after enzymatic activation or incubation in buffer alone, with the following sets of parameters:

- Ex 400 nm (slit 5 nm), Em 410–750 nm (slit 5 nm),
- Ex 420 nm (slit 5 nm), Em 450–750 nm (slit 5 nm),
- Ex 500 nm (slit 5 nm), Em 510–850 nm (slit 12 nm).

RP-HPLC-fluorescence and RP-HPLC-MS (full scan and SIM modes) analyses

Enzymatic reaction mixtures from fluorescence-based *in vitro* assays were firstly analyzed by RP-HPLC-fluorescence (injected volume: 20 μL, system H) and then by RP-HPLC-MS (injected volume: 20 μL, system I without fluorescence detection but with UV-vis detection at 220, 400, 475 and 520 nm and mass detection (full scan in both ESI+/-, 100–1500 a.m.u., and SIM modes for mass detection, SIM width: 1 a.m.u)). In some cases, samples have been frozen with liquid nitrogen and stored at −25 °C. Defrosting and subsequent RP-HPLC analyses were considered only when instrument was available.

Please note: injection of buffer (Tris.HCl buffer) was also achieved immediately prior to each SIM analysis, especially to confirm the lack of residual contaminants within the C_{18} column or ESI probe at the corresponding m/z value selected for the SIM detection mode and then avoid misinterpretations.

In vitro Activation of PPi-Responsive Coumarin-Salen Fe(III) Complex 18

Experimental details about stock solutions of probe and PPi anion, and buffer

- 1.0 mg/mL stock solutions of PPi-responsive probe **18** (1.2 mM) was prepared in DMSO (UV-spectroscopy grade, Honeywell Riedel-de-Haën).
- 10.0 mg/mL stock solution of NaPPi .10 H_2O (Prolabo) was prepared in ultrapure water (22.4 mM).
- HEPES buffer (20 mM, pH 7.5) prepared in ultrapure H_2O.

Fluorescence-based assays

All assays were performed at 25 °C (using a Lauda Ecoline Recirculating Chiller RE 106 combined with a temperature controller Lauda E100, connected to the spectrofluorometer cell holder) and conducted with magnetic stirring. Probe's concentration in 3.5 mL fluorescence quartz cell was set to 1.0 μM. The volume of the probe's solution was always 3.0 mL. The following set of detection parameters was used: Ex/Em 390/515, slits 3 nm. Fluorescence emission of released coumarin **3** was monitored at this Ex/Em wavelength pair, over time with measurements every 5 s (duration of assay: 9 h30). 100 equiv. (13.34 μL) of NaPPi solution was added after 5 min (10 equiv.), then 17 min (90 equiv.) of incubation in buffer.

Acknowledgements

This work is part of the project "MULTIMOD", supported by the Conseil Régional de Bourgogne Franche-Comté and the European Union through the PO FEDER-FSE Bourgogne 2014/2020 programs. Financial supports from Agence Nationale de la Recherche (ANR, AAPG 2018, PRCI, LuminoManufacOligo, ANR-18-CE07-0045; AAPG 2021, PRC, InnoTherano, ANR-21-CE07-0010), especially for the post-doc fellowship of Dr. Kévin Renault (2019-2021, 29 months) and for the purchase of InGaAs single channel detector, and ADEME (Agence de la transition écologique) and AID (Agence de l'Innovation de Défense) for the Ph.D. grant of Vincent Gaumerd (2023-2026, 36 months) are greatly acknowledged. GDR CNRS "Agents d'Imagerie Moléculaire" (AIM) 2037 is also thanked for its interest in this work. The authors (affiliated to ICMUB lab) thank the "Plateforme d'Analyse Chimique et de Synthèse Moléculaire de l'Université de Bourgogne" (PACSMUB, http://www.wpcm.fr) for access to analytical and molecular spectroscopy instruments. The authors (affiliated to ICMUB lab) also thank Dr. Myriam Laly (University of Burgundy, PACSMUB) for the determination of TFA content in fluorophore/probe samples, Mrs. Tiffanie Régnier (SATT SAYENS, PACSMUB) for elemental analyses, Mr. Cédric Balan (University of Burgundy, ICMUB, PACSMUB) for Karl Fischer titrations, Dr. Valentin Quesneau (UBFC, ICMUB, 2019–2021) for the purification of commercial 4-(diethylamino)salicylaldehyde, Dr. Gilles Ulrich (ICPEES, UMR 7515, Strasbourg) for fruitful discussion on spectral behavior of compounds **2** and **3**, and Porphychem company for the generous gift of ZnTPP.

Conflict of Interests

The authors declare no conflict of interest.

Data Availability Statement

The data that support the findings of this study are available from the corresponding author upon reasonable request.

Keywords: *N*-alkylpyridinium salt · coumarin · covalent-assembly · fluorescent probe · molecular disassembly · *ortho*-salicylaldehyde

[1] For selected reviews, see: a) S. Singha, Y. W. Jun, S. Sarkar, K. H. Ahn, *Acc. Chem. Res.* **2019**, *52*, 2571–2581; b) K. J. Bruemmer, S. W. M. Crossley, C. J. Chang, *Angew. Chem. Int. Ed.* **2020**, *59*, 13734–13762; c) J. V. Jun, D. M. Chenoweth, E. J. Petersson, *Org. Biomol. Chem.* **2020**, *18*, 5747–5763; d) A. K. East, M. Y. Lucero, J. Chan, *Chem. Sci.* **2021**, *12*, 3393–3405; e) H. Li, D. Kim, Q. Yao, H. Ge, J. Chung, J. Fan, J. Wang, X. Peng, J. Yoon, *Angew. Chem. Int. Ed.* **2021**, *60*, 17268–17289.

[2] For selected reviews, see: a) H. E. Katerinopoulos, *Curr. Pharm. Des.* **2004**, *10*, 3835–3852; b) H. Li, L. Cai, Z. Chen, in *Advances in Chemical Sensors* (Ed.: W. Wang), InTech, **2011**, pp. 121–150; c) D. Cao, Z. Liu, P. Verwilst, S. Koo, P. Jangjli, J. S. Kim, W. Lin, *Chem. Rev.* **2019**, *119*, 10403–10519; d) A. Mondal, S. Nag, P. Banerjee, *Dalton Trans.* **2021**, *50*, 429–451; e) G. Tian, Z. Zhang, H. Li, D. Li, X. Wang, C. Qin, *Crit. Rev. Anal. Chem.* **2021**, *51*, 565–581; f) Pooja, H. Pandey, S. Aggarwal, M. Vats, V. Rawat, S. R. Pathak, *Asian J. Org. Chem.* **2022**, *11*, e202200455; g) D. Khan, Shaily, *Appl. Organomet. Chem.* **2023**, *37*, e7138.

[3] For the popular example of 4-methylumbelliferyl phosphate (4-MUP), embedded in VIDAS® immunoassays (bioMérieux), see: H. Fernley, P. Walker, *Biochem. J.* **1965**, *97*, 95–103.

[4] For reviews, see: a) S. J. Sharma, N. Sekar, *Dyes Pigm.* **2022**, *202*, 110306; b) Y. Fan, Y. Wu, J. Hou, P. Wang, X. Peng, G. Ge, *Coord. Chem. Rev.* **2023**, *480*, 215020.

[5] a) W.-X. Sun, N. Li, Z.-Y. Li, Y.-C. Yuan, J.-Y. Miao, B.-X. Zhao, Z.-M. Lin, *Dyes Pigm.* **2020**, *182*, 108658; b) Y. Du, F. Li, S. Sun, B. Zhao, *J. Fluoresc.* **2022**, *32*, 2151–2157; c) F. Li, W. Yao, C.-H. Tian, Y.-F. Du, J.-Z. Wang, T.-Y. Zhang, J.-Y. Miao, B.-X. Zhao, *Spectrochim. Acta Part A* **2022**, *271*, 120870; d) S. Sarkar, A. Shil, M. Nandy, S. Singha, Y. J. Reo, Y. J. Yang, K. H. Ahn, *Anal. Chem.* **2022**, *94*, 1373–1381.

[6] O. S. Wolfbeis, H. Marhold, *Chem. Ber.* **1985**, *118*, 3664–3672.

[7] a) W. Gross, W. Benicke, D. Fuhr, A. Kleen, (Henkel AG & Co. KGaA), DE102008018132, **2009**; b) W. Gross, W. Benicke, D. Fuhr, A. Kleen, (Henkel AG & Co. KGaA), WO2009124800, **2009**.

[8] Z. Liang, Y. Sun, R. Duan, R. Yang, L. Qu, K. Zhang, Z. Li, *Anal. Chem.* **2021**, *93*, 12434–12440.
[9] a) S. Sowmiah, J. M. S. S. Esperança, L. P. N. Rebelo, C. A. M. Afonso, *Org. Chem. Front.* **2018**, *5*, 453–493; b) G. Aragay, P. Ballester, *Isr. J. Chem.* **2024**, *in press*, e202300041.
[10] a) H. Zhu, J. Fan, J. Du, X. Peng, *Acc. Chem. Res.* **2016**, *49*, 2115–2126; b) M. K. Goshisht, N. Tripathi, G. K. Patra, M. Chaskar, *Chem. Sci.* **2023**, *14*, 5842–5871.
[11] a) D. V. Berdnikova, E. Y. Chernikova, *ChemPhotoChem* **2024**, *in press*, e202300140; b) S. Chatterjee, F. Liang, *ChemistrySelect* **2023**, *8*, e202204833; c) X. Kang, A. Ahmad Dar, R. Reddy Mittapalli, A. Carrao, A. Dawn, H. Kumari, *ChemistrySelect* **2023**, *8*, e202300894.
[12] a) Q. Wu, E. V. Anslyn, *J. Mater. Chem.* **2005**, *15*, 2815–2819; b) *J. Am. Chem. Soc.* **2010**, *132*, 15833–15835; c) Y. Yang, S. K. Seidlits, M. M. Adams, V. M. Lynch, C. E. Schmidt, E. V. Anslyn, J. B. Shear, *J. Am. Chem. Soc.* **2010**, *132*, 13114–13116.
[13] a) F. Zelder, *Chem. Eur. J.* **2024**, in press, e202302705; b) P. Yadav, F. Zelder, *Chimia* **2020**, *74*, 252–256.
[14] T. V. Hansen, L. Skattebøl, *Org. Synth.* **2005**, pp. 64–68, DOI: https://doi.org/10.1002/0471264229.os082.10.
[15] A. Rieche, H. Gross, E. Höft, in *Organic Syntheses, Vol. 49*, **1967**, pp. 1–3, DOI: 10.15227/orgsyn.047.0001.
[16] B. Roubinet, P.-Y. Renard, A. Romieu, *Dyes Pigm.* **2014**, *110*, 270–284.
[17] A. M. Brouwer, *Pure Appl. Chem.* **2011**, *83*, 2213–2228.
[18] K.-i. Setsukinai, Y. Urano, K. Kikuchi, T. Higuchi, T. Nagano, *J. Chem. Soc. Perkin Trans. 2* **2000**, 2453–2457.
[19] Y. Hu, L. Ma, Z. Zhang, Y. Huang, H. Zhang, J. Wu, C. Liu, *J. Photochem. Photobiol. A* **2023**, *445*, 115082.
[20] A. A. Krasnovsky Jr, *Photochem. Photobiol.* **1979**, *29*, 29–36.
[21] R. Schmidt, H. D. Brauer, *J. Am. Chem. Soc.* **1987**, *109*, 6976–6981.
[22] R. W. Redmond, J. N. Gamlin, *Photochem. Photobiol.* **1999**, *70*, 391–475.
[23] M. V. Encinas, E. Lemp, E. A. Lissi, *J. Chem. Soc. Perkin Trans. 2* **1987**, *2*, 1125–1127.
[24] M. Elsherbini, R. K. Allemann, T. Wirth, *Chem. Eur. J.* **2019**, *25*, 12486–12490.
[25] a) U. Mazzucato, G. G. Aloisi, F. Masetti, *J. Photochem.* **1982**, *18*, 211–222; b) A. Chmyrov, T. Sandén, J. Widengren, *J. Phys. Chem. B* **2010**, *114*, 11282–11291; c) S. Li, X. Jin, Z. Zhang, J. Li, J. Hua, *Mater. Chem. Front.* **2023**, *7*, 3738–3746.
[26] M. S. Baptista, J. Cadet, P. Di Mascio, A. A. Ghogare, A. Greer, M. R. Hamblin, C. Lorente, S. C. Nunez, M. S. Ribeiro, A. H. Thomas, M. Vignoni, T. M. Yoshimura, *Photochem. Photobiol.* **2017**, *93*, 912–919.
[27] J. R. Lakowicz, S. Keating-Nakamoto, *Biochemistry* **1984**, *23*, 3013–3021.
[28] L. Yan, C. Zhou, H. Yang, *Sens. Actuators B* **2023**, *382*, 133492.
[29] J. Morgan, A. R. Oseroff, *Adv. Drug. Deliver.* **2001**, *49*, 71–86.
[30] Y. Guo, W. Liu, J. Sha, X. Li, H. Ren, J. Wu, W. Zhang, C.-S. Lee, P. Wang, *Spectrochim. Acta Part A* **2023**, *296*, 122698.
[31] For selected reviews, see: a) X. Chen, M. Sun, H. Ma, *Curr. Org. Chem.* **2006**, *10*, 477–489; b) C. R. Drake, D. C. Miller, E. F. Jones, *Curr. Org. Synth.* **2011**, *8*, 498–520; c) J. B. Grimm, L. M. Heckman, L. D. Lavis, in *Progress in Molecular Biology and Translational Science, Vol. 113* (Ed.: M. C. Morris), Academic Press, **2013**, pp. 1–34; d) W. Chyan, R. T. Raines, *ACS Chem. Biol.* **2018**, *13*, 1810–1823.
[32] X. Wu, W. Shi, X. Li, H. Ma, *Acc. Chem. Res.* **2019**, *52*, 1892–1904.
[33] Y. Tang, D. Lee, J. Wang, G. Li, J. Yu, W. Lin, J. Yoon, *Chem. Soc. Rev.* **2015**, *44*, 5003–5015.
[34] X. Luo, L. Gu, X. H. Qian, Y. C. Yang, *Chem. Commun.* **2020**, *56*, 9067–9078.
[35] T.-H. Kim, T. M. Swager, *Angew. Chem. Int. Ed.* **2003**, *42*, 4803–4806.
[36] For reviews, see: a) X. Chen, Z. Huang, L. Huang, Q. Shen, N.-D. Yang, C. Pu, J. Shao, L. Li, C. Yu, W. Huang, *RSC Adv.* **2022**, *12*, 1393–1415; b) A. Romieu, *Org. Biomol. Chem.* **2015**, *13*, 1294–1306; c) P. Zhang, Q. Zhang, L. Zhang, H. Zhong, C. Ding, *TrAC Trends Anal. Chem.* **2020**, *123*, 115776.
[37] a) P. Kundu, K. C. Hwang, *Anal. Chem.* **2012**, *84*, 4594–4597; b) Y. Hao, T. Li, L. Luo, S. Fan, S. Chen, Y. Zhang, Z. Tang, M. Xu, R. Zeng, S. Chen, *Sens. Actuators B* **2022**, *369*, 132405; c) T. Li, Y. Hao, H. Dong, C. Li, J. Liu, Y. Zhang, Z. Tang, R. Zeng, M. Xu, S. Chen, *ACS Sens.* **2022**, *7*, 415–422; d) X. Rong, Y. Peng, C. Liu, M. Li, J. Shi, M. Yu, S. Ba, W. Sheng, B. Zhu, *New J. Chem.* **2022**, *46*, 23096–23101; e) C. Yu, S. Wang, C. Xu, Y. Ding, G. Zhang, N. Yang, Q. Wu, Q. Xiao, L. Wang, B. Fang, C. Pu, J. Ge, L. Gao, L. Li, S. Q. Yao, *Adv. Healthcare Mater.* **2022**, *11*, 2200400; f) J. Chang, Y. Wang, H. Wei, X. Kong, B. Dong, T. Yue, *Spectrochim. Acta Part A* **2023**, *302*, 123080; g) Y.-C. Ku, P.-H. Lin, C.-Y. Huang, C.-W. Lee, C.-H. Yu, S.-C. Chen, W.-M. Liu, *Dyes Pigm.* **2023**, *210*, 111004; h) D. Li, S. Tu, Y. Le, Y. Zhou, L. Yang, Y. Ding, L. Huang, L. Liu, *Spectrochim. Acta Part A* **2023**, *285*, 121816; i) D. Li, S. Tu, Y. Le, Y. Zhou, L. Yang, Y. Ding, L. Huang, L. Liu, *Chem. Pap.* **2023**, *77*, 1741–1749; j) M. Sang, Y. Huang, Z. Liu, G. Li, Y. Wang, Z. Yuan, C. Dai, J. Zheng, *ACS Sens.* **2023**, *8*, 893–903; k) Z. Y. Xu, X. H. Wang, H. Q. Luo, N. B. Li, *Food Chem.* **2023**, *407*, 135120; l) Y. Yang, M. Ma, L. Shen, J. An, E. Kim, H. Liu, M. Jin, S. Wang, J. Zhang, J. S. Kim, C. Yin, *Angew. Chem. Int. Ed.* **2023**, *62*, e202310408; m) Y. Yang, K. Zhou, M. Ma, H. Liu, M. Jin, C. Yin, S. Wang, J. Zhang, *Chem. Eng. J.* **2023**, *452*, 139020.
[38] a) W. Feng, C. Gao, W. Liu, H. Ren, C. Wang, K. Ge, S. Li, G. Zhou, H. Li, S. Wang, G. Jia, Z. Li, J. Zhang, *Chem. Commun.* **2016**, *52*, 9434–9437; b) W. Liu, H. Liu, X. Peng, G. Zhou, D. Liu, S. Li, J. Zhang, S. Wang, *Bioconjugate Chem.* **2018**, *29*, 3332–3343; c) X. Peng, J. Gao, Y. Yuan, H. Liu, W. Lei, S. Li, J. Zhang, S. Wang, *Bioconjugate Chem.* **2019**, *30*, 2828–2843; d) N. Singh, A. Gupta, P. Prasad, R. K. Sah, A. Singh, S. Kumar, S. Singh, S. Gupta, P. K. Sasmal, *J. Med. Chem.* **2021**, *64*, 17813–17823; e) A. Gupta, N. Singh, A. Gautam, N. Dhakar, S. Kumar, P. K. Sasmal, *RSC Med. Chem.* **2023**, *14*, 1088–1100.
[39] S. Debieu, A. Romieu, *Org. Biomol. Chem.* **2015**, *13*, 10348–10361.
[40] J. Yan, S. Lee, A. Zhang, J. Yoon, *Chem. Soc. Rev.* **2018**, *47*, 6900–6916.
[41] K. Wang, W. Wang, X.-Y. Zhang, A.-Q. Jiang, Y.-S. Yang, H.-L. Zhu, *TrAC Trends Anal. Chem.* **2021**, *136*, 116189.
[42] J. Park, Y. Kim, *Bioorg. Med. Chem. Lett.* **2013**, *23*, 2332–2335.
[43] For selected reviews, see: a) H. C. Kang, *Biomaterials* **2018**, *22*, 34; b) H. Singh, D. Sareen, J. M. George, V. Bhardwaj, S. Rha, S. J. Lee, S. Sharma, A. Sharma, J. S. Kim, *Coord. Chem. Rev.* **2022**, *452*, 214283.
[44] For selected reviews, see: a) S. K. Kim, D. H. Lee, J.-I. Hong, J. Yoon, *Acc. Chem. Res.* **2009**, *42*, 23–31; b) S. Lee, K. K. Y. Yuen, K. A. Jolliffe, J. Yoon, *Chem. Soc. Rev.* **2015**, *44*, 1749–1762; c) J. Wongkongkatep, A. Ojida, I. Hamachi, *Top. Curr. Chem.* **2017**, *375*, 30.
[45] a) N. Kumari, F. Zelder, *Chem. Commun.* **2015**, *51*, 17170–17173; b) N. Kumari, H. Huang, H. Chao, G. Gasser, F. Zelder, *ChemBioChem* **2016**, *17*, 1211–1215; c) P. Yadav, M. Jakubaszek, B. Spingler, B. Goud, G. Gasser, F. Zelder, *Chem. Eur. J.* **2020**, *26*, 5717–5723; d) P. Yadav, O. Blacque, A. Roodt, F. Zelder, *Inorg. Chem. Front.* **2021**, *8*, 4313–4323; e) S. Bohnhoff-Müller, P. Yadav, B. Spingler, O. Blacque, F. Zelder, *J. Porphyrins Phthalocyanines* **2023**, *27*, 661–669.
[46] D. Winkler, S. Banke, P. Kurz, *Z. Anorg. Allg. Chem.* **2020**, *646*, 933–939.
[47] E. Y.-L. Hui, D. W. P. Taiy, J.-A. Richard, Z. Pohancenikova, K. Renault, A. Romieu, Y.-H. Lim, *Dyes Pigm.* **2022**, *207*, 110708.
[48] A. Gualandi, M. Marchini, L. Mengozzi, H. T. Kidanu, A. Franc, P. Ceroni, P. G. Cozzi, *Eur. J. Org. Chem.* **2020**, *2020*, 1486–1490.
[49] a) W. Chen, X. Ma, H. Chen, S. Hua Liu, J. Yin, *Coord. Chem. Rev.* **2021**, *427*, 213584; b) L. Zhang, F.-L. Jiang, Q.-L. Guo, Y. Liu, P. Jiang, *Anal. Chem.* **2022**, *94*, 4126–4133.
[50] T.-W. Wu, F.-H. Lee, R.-C. Gao, C. Y. Chew, K.-T. Tan, *Anal. Chem.* **2016**, *88*, 7873–7877.
[51] K. Renault, Y. Capello, S. Yao, S. Halila, A. Romieu, *Chem. Asian J.* **2023**, *18*, e202300258.
[52] H. Mohapatra, H. Kim, S. T. Phillips, *J. Am. Chem. Soc.* **2015**, *137*, 12498–12501.
[53] F. Biedermann, in *Supramolecular Chemistry in Water* (Ed.: S. Kubik), Wiley-VCH, Weinheim, **2019**, pp. 35–77.
[54] H. Shen, C. Liu, J. Zheng, Z. Tao, H. Nie, X.-L. Ni, *ACS Appl. Mater. Interfaces* **2021**, *13*, 55463–55469.
[55] G. R. Fulmer, A. J. M. Miller, N. H. Sherden, H. E. Gottlieb, A. Nudelman, B. M. Stoltz, J. E. Bercaw, K. I. Goldberg, *Organometallics* **2010**, *29*, 2176–2179.
[56] G. Dejouy, M. Laly, I. E. Valverde, A. Romieu, *Dyes Pigm.* **2018**, *159*, 262–274.
[57] Y. Hu, Z. Chen, L. Ma, Z. Zhang, H. Zhang, F. Yi, C. Liu, *Tetrahedron* **2022**, *117–118*, 132837.

Manuscript received: December 1, 2023
Revised manuscript received: January 8, 2024
Accepted manuscript online: January 9, 2024
Version of record online: January 30, 2024